EVALUATION OF THE EFFECTS OF INTELLIGENT CRUISE CONTROL VEHICLES IN MIXED TRAFFIC[1]

Petros Ioannou

Center for Advanced Transportation Technologies

Dept. of Electrical Engineering-Systems, EEB200A

University of Southern California

Los Angeles, CA 90089-2562, USA

ioannou@usc.edu

Final Report for Task Order 4217 (former MOU 392)

September 2002

[1] This work is supported by the California Department of Transportation through PATH of the University of California. The contents of this report reflect the views of the authors who are responsible for the facts and accuracy of the data presented herein. The contents do not necessarily reflect the official views or policies of the State of California or the Federal Highway Administration. This report does not constitute a standard, specification or regulation.

Executive Summary

This is the final report for the project entitled "Evaluation of the Effects of Intelligent Cruise Control Vehicles in Mixed Traffic". The project was initially under MOU392 and switched to Task Order 4217 at the beginning of the 2nd year of the project. Due to this administrative change a final report was submitted to PATH for MOU392 covering all the tasks completed during the 1st year of the project. The two research tasks that were not completed under MOU392 became the main focus of Task Order 4217. These research tasks are described below:

Task 1: Lane change and cut-ins

The Tasks under MOU392 covered the properties of mixed traffic in a single lane without taking into account lane changes. Large intervehicle spacing created by the ICC vehicle when the lead manual vehicle accelerates rapidly may invite lane changes or cut-ins from vehicles in neighboring lanes that may adversely affect traffic flow. These disturbances may also affect the environmental benefits calculated under the tasks of MOU392. In this Task we examine the effects of lane changes and cut-ins on the transient behavior of vehicles in mixed traffic as well as on the macroscopic behavior of traffic flow. Some lane changing experiments involving ICC vehicles will also be performed to collect data about possible disturbances and transients.

Task 2: Macroscopic analysis of mixed traffic

Under this Task we plan to use the fundamental flow-density and space-time diagrams to study the macroscopic properties of mixed traffic that involves ICC and manual vehicles. The experimental data and results obtained under the Tasks of MOU392 will be used to come up with more realistic vehicle response characteristics for macroscopic analysis. The main objective of this Task is to develop a better understanding of the macroscopic behavior of mixed ICC/manual vehicles.

The results obtained for task 1, 2 above are presented in Chapters I and II respectively. The report on Task 2 has already been submitted and published as a PATH report. The report on Task 1 will also be submitted to be published as an independent PATH report. The main findings of Task Order 4217 are summarized below and presented in detailed in the two appendices.

We demonstrate using theory, simulations and experiments that during lane changes, the smoothness of the adaptive cruise control (ACC) (also referred to as intelligent cruise control (ICC)) vehicle response attenuates the disturbances introduced by the cut –in or exiting vehicle in a way that is beneficial to the environment when compared with similar situations where the ACC vehicle is absent. We concluded that the higher number of possible cut-ins that may be present due to the higher gaps created during high accelerations maneuvers by the vehicle in front of the ACC vehicle, will not take away the benefits shown in the absence of such cut –ins when compared with the situation of similar maneuvers but with no cut-ins in the case of 100% manually driven vehicles. We generated several sensitivity curves that show how the improvements in emissions and fuel economy vary with the level of disturbances, penetration of ACC vehicles and other

variables. Because the magnitude of these improvements depends on the type of disturbances generated, and on the model characteristics of the human driver models used it is difficult to assess quantitatively the effect ACC vehicles will have in a complex highway system. One could easily argue that a human driver could drive as smoothly as the ACC system on the vehicle producing similar effects and benefits. While this may be true for some drivers the large majority drive in a way that their response is accurately captured by the human driver model used in this study which by the way was validated using actual experiments as part of MOU392.

The macroscopic analysis of mixed manual/semi-automated traffic is presented in Chapter II. We focus our analysis on two topics: the fundamental traffic flow-density diagram and traffic flow disturbances such as shock waves. We derive the fundamental traffic flow-density diagram for mixed manual/semi-automated traffic using the traffic flow-density diagrams for 100% manual and 100% semi-automated traffic. We show in a graphical way and demonstrate using simulations the effect of semi-automated vehicles on mixed traffic flow during the presence of disturbances such as shock waves. Lastly we show using queuing theory the effect of semi-automated vehicles on the average delay and number of vehicles in a queue on the highway during the presence of shock waves that produce stop-and-go traffic. We showed that the presence of ACC vehicles will attenuate shock waves and pass them on to the vehicles upstream in a much faster way than in the case of manual vehicles due to the shorter reaction times that characterizes the ACC vehicle. This implies that the shock wave will get dissipated faster as it will reach low density regions or the entrances to the highway faster in the presence of ACC vehicles than in the case of 100% manual vehicles.

The overall conclusion is that ACC vehicles will have beneficial effects on the environment and traffic flow characteristics overall as they penetrate the traffic network.

Contents

List of Figures

List of Tables

CHAPTER I

EVALUATION OF THE ACC VEHICLES IN MIXED TRAFFIC: LANE CHANGE EFFECTS AND SENSITIVITY ANALYSIS

by
Petros Ioannou and Margareta Stefanovic

Abstract

Almost every automobile company is producing vehicles with Adaptive Cruise Control (ACC) systems that allow a vehicle to do automatic vehicle following in the same lane. The ACC system is designed for driver comfort and safety and to operate with manually driven vehicles. These characteristics of ACC were found to have beneficial effects on the environment and traffic flow characteristics [1, 2, 3] by acting as filters of a wide class of traffic disturbances. It has been argue that the smooth response of ACC vehicles to high acceleration disturbances or large position errors creates large gaps between the ACC vehicle and the vehicle ahead inviting cut –ins and therefore generating additional disturbances that would not have been created if the vehicles were all manually driven.

In this Chapter we examine the effect of lane changes on the benefits suggested in [1,2,3] as well as the sensitivity of these benefits with respect to various variables such as ACC penetration, level of traffic disturbances etc. We demonstrate using theory, simulations and experiments that during lane changes, the smoothness of the ACC vehicle response attenuates the disturbances introduced by the cut –in or exiting vehicle in a way that is beneficial to the environment when compared with similar situations where the ACC vehicle is absent. We concluded that the higher number of possible cut-ins that may be present due to the higher gaps created during high accelerations maneuvers by the vehicle in front of the ACC vehicle, will not take away the benefits shown in the absence of such cut –ins when compared with the situation of similar maneuvers but with no cut-ins in the case of 100% manually driven vehicles.

I-1 Introduction

Recent advances in technology have propelled efforts to automate vehicles in order to achieve safe and efficient use of the current highway system. Fully automated vehicles that are able to operate autonomously in a highway environment are a long-term goal. On the other hand, partially or semi-automated vehicles designed to operate with current manually driven vehicles in today's highway traffic are seen as a more near term objective. Adaptive Cruise Control (ACC) systems developed during the last decade and recently produced and made available to users by every major automobile company is the first step towards that direction.

Considering the current penetration of products such as Anti-Lock Braking Systems (ABS), air bags and cruise control into the vehicle market, it is justifiable to expect that ACC systems that give vehicles the capability to follow the vehicle in front automatically

in the same lane will penetrate the market in a similar fashion. A variety of different ACC control schemes have been designed for passenger cars during the last decade. Human factors and driver comfort considerations dictate that the response of the ACC vehicle to a leading vehicle maneuver or disturbance should be smooth. This smooth response of the ACC vehicle was suspected to have beneficial effects on traffic flow characteristics and the environment. Since the vehicle-highway system is one of the major contributors to air pollution in urban areas due to increasing vehicle miles traveled and congestion [8], the impact of the ACC vehicles on the environment as more of these vehicles penetrate the system is an important topic for investigation and it was first addressed in [3].

In [1-3] the effects of ACC vehicles operating together with manually driven vehicles in a mixed traffic situation are analyzed on the microscopic and macroscopic level using the fundamental diagram, space-time graphs and simulations. The results of the analysis that are demonstrated experimentally on the microscopic level indicate that ACC vehicles have a beneficial effect on traffic flow characteristics and positive effects on the environment due to their smoother response and more intelligent use of the throttle and brake in achieving desired driving tasks in situations involving high acceleration maneuvers.

The results of [1] developed using simulations and experiments show that a disturbance generated by vehicle during a high acceleration maneuver is attenuated when it reaches an ACC vehicle due to the fact that the ACC vehicle is designed to respond to such disturbances in a smooth way and with lower acceleration. While this characteristic of the ACC vehicle has beneficial effects on the environment and traffic flow characteristics in the same lane, the analysis and study of [1-3] does not include the effect of this ACC response to the vehicles in the neighboring lane. For example a rapidly accelerating vehicle in front of the ACC vehicle will create a large gap between the two vehicles since the ACC vehicle will follow such a vehicle with much lower acceleration due to human factors and driver comfort constraints. Such a large gap may invite vehicles from neighboring lanes to cut in. As a result additional disturbances will be created that have not been taken into account in the work of [1-3]. Similarly lane exit may also generate disturbances. A vehicle ahead of ACC may change lanes for several reasons but one possible reason could be that the driver of such vehicle does not want to be followed by a vehicle driven by the computer. While this assumption may not be valid with the current ACC designs where relatively large minimum time headways are used, it may be valid in the case of future more advanced ACC systems with much smaller minimum time headways.

The purpose of this Chapter is to first examine the sensitivity of earlier results obtained in [1] with respect to several variables such as level of disturbance, percent penetration of the ACC vehicles etc, and evaluate the effect of lane changes on traffic flow characteristics on the microscopic level and environment.

I-2 ACC vehicle behavior in mixed traffic

In [1,3] it was established using theory and experiments that ACC vehicles have beneficial effects on traffic flow characteristics and the environment especially during disturbances generated when the lead vehicle in front of the ACC vehicle exhibits high acceleration maneuvers. The emission model developed in [5,6] is used to calculate the benefits in terms of pollution benefits and fuel economy. The reason why the ACC vehicle response is so friendly to the environment is that ACC vehicles are designed to exhibit smooth response to changes in speed and acceleration mainly for human factors and driver comfort purposes. The results in [1] are demonstrated experimentally at Richmond Field and Crows Landing and they are found to be in close agreement with those predicted from theory and simulations using driver and ACC models. In [1] the ACC vehicle was always at a position close to the point where the disturbance was generated, followed by a number of human driven vehicles. The sensitivity of the benefits generated in [1] with respect to the position of the ACC vehicle in the string of a number of vehicles and to other variables is examined in this section.

I-2.1 High acceleration maneuvers

Let us consider a string of ten vehicles following one another in the same lane. Due to an accident that was just cleared, the lead vehicle begins to accelerate from 0 speed with acceleration 0.35g to 24.5 m/s. The rest of the vehicles respond accordingly trying to follow the vehicle response of the vehicle right in front of them in an effort to maintain a small but comfortable intervehicle spacing. After reaching 24.5 m/s, the lead vehicle decelerates to 14.5 m/s at –0.3g, and finally accelerates back to 24.5 m/s at the acceleration rate of 0.25g.

In order to examine the effect of these maneuvers on the environment and the difference between having an ACC vehicle present in the string of the 10 vehicles and not having one we use as in [1] the Pipes model [4] to model human drivers and the ACC model [7] to model the ACC vehicle. Figure I-1 shows the speed responses of the various vehicles in the string of 10 when all vehicles are manually driven. As indicated in [1,3] the disturbance generated by the lead vehicle gets amplified and becomes more oscillatory as it travels upstream. This is a phenomenon often observed in today's traffic. In Figure I-2 we assume that the 4^{th} vehicle in the string of 10 is an ACC vehicle. It follows from Figure I-2 that the ACC vehicle due its limited acceleration cannot follow the rapid oscillatory speed response of the vehicle in front but instead it acts as a filter presenting to the vehicles behind a smoother less oscillatory speed response to follow. The drawback of this ACC behavior is that the intervehicle spacing between the ACC vehicle and that in front becomes large for some time until the ACC vehicle catches up as shown in Figure I-3. In some cases if the vehicle ahead of the ACC continues speeding with high acceleration the ACC vehicle may lose the target and switch to the cruise mode.

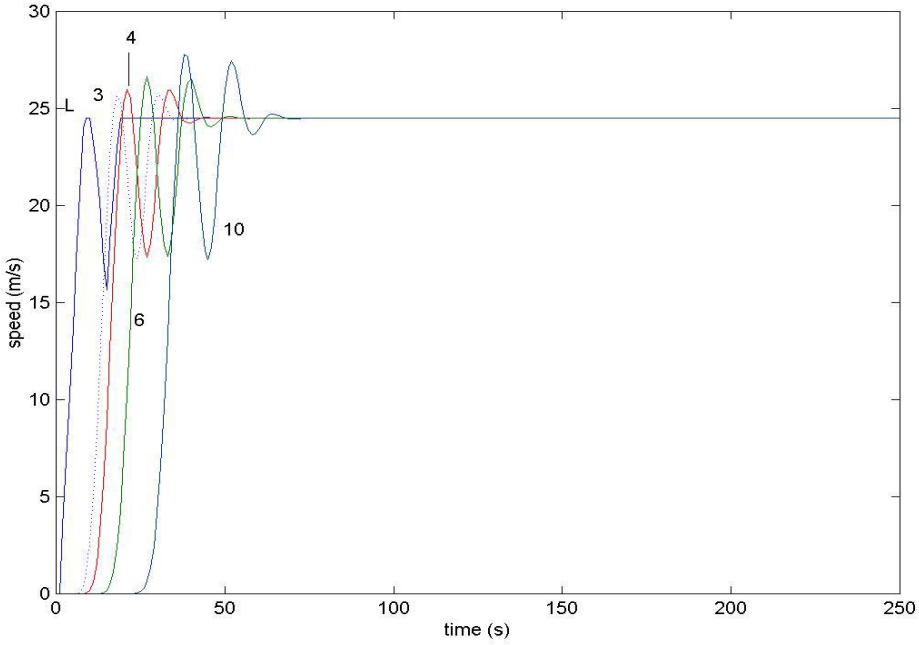

Figure I-1: High acceleration/deceleration maneuver initiated by the lead vehicle; Speed responses of the lead, 3rd, 4th, 6th and 10th vehicle in a string of 10 manually driven vehicles

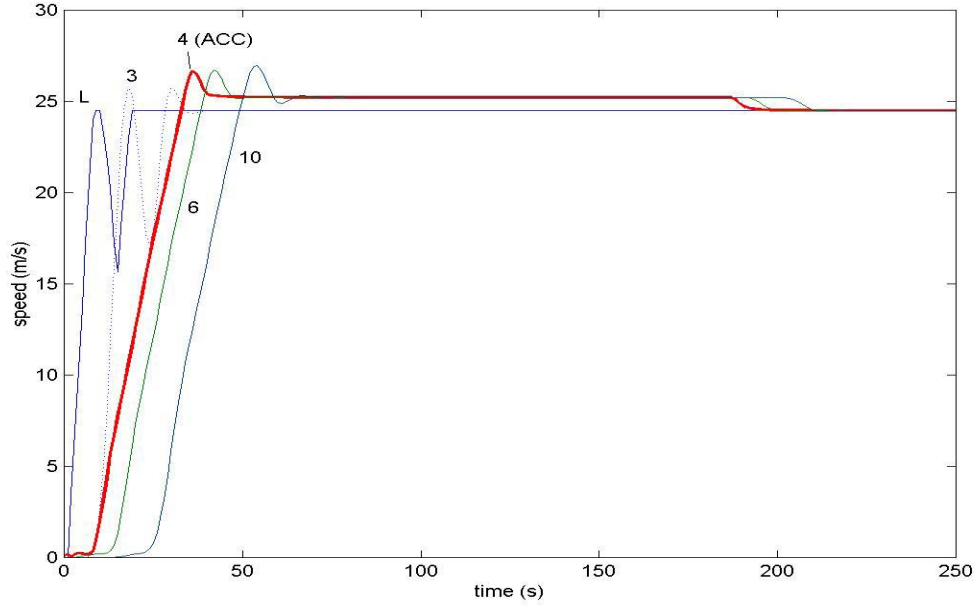

Figure I-2: High acceleration/deceleration maneuver initiated by the lead vehicle; Speed responses of the 1st, 3rd, 4th, 6th and 10th vehicle in a string of 10 vehicles of which the 4th is ACC and the rest are manually driven.

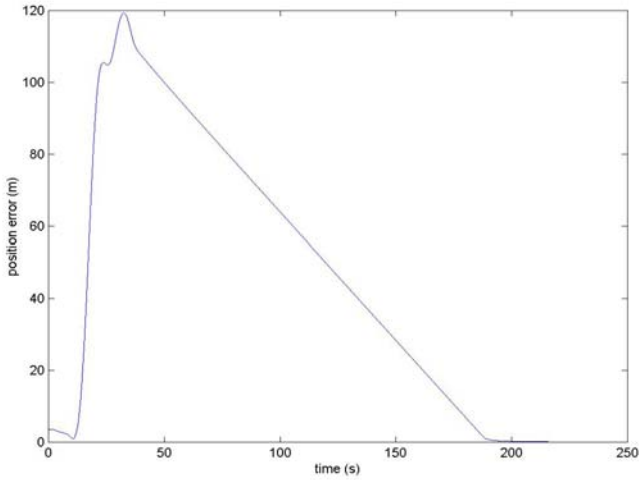

Figure I-3: Large Position error for the ACC vehicle due to its limited acceleration

As analyzed in [1], the above simulations show that the smooth response of the ACC vehicles have beneficial effects on the environment and fuel economy. Using the emissions model of [5,6] we compare the accumulative pollution levels and fuel economy for the case where the 10 vehicles are manually driven and when the 4th vehicle in the string of 10 is replaced with an ACC vehicle for the same lead vehicle maneuver. The results are summarized in table 1.

Table 1. Summary of benefits

	Percent benefits of mixed over manual traffic in high acceleration vehicle following
HC emission	38 %
CO emission	48 %
CO_2 emission	negligible
Fuel consumption	8 %

The above results are in agreement with those presented in [1]. In [1] the validity of the above results is demonstrated experimentally using 3 vehicles. Due to the short range of the ranging sensor, high accelerations were not possible as at such accelerations large gaps are created and the ACC vehicle loses the target forcing it to switch to the cruise mode. As a result these experiments are repeated with a longer range sensor as described in the following subsection.

I-2.2 Experiments

Several runs of tests were performed at the Crows Landing test track with the aim of investigating the validity of the theoretical results. They consisted of two types of traffic – fully manual in which all vehicles were under manual control and mixed in which one of the vehicles was equipped with an ACC system and the rest were manually driven. Three vehicles were used for the experiments, with one changing to the ACC mode for the mixed traffic scenarios.

The ACC system was implemented on a Buick LeSabre experimental vehicle .The ACC controller used range and range rate measurements from the radar mounted at the front of the vehicle. The experimental vehicle had two radars installed: Doppler Eaton-Vorad EV300 radar, with more than 150m range and a non-Doppler Delco radar, with shorter range of ~50m. Most of the time, the radar reading used by the controller was that of EV-300. However, due to the fact that it is a Doppler type radar, when the relative velocity was less than 0.25 mph the radar range reading dropped to zero. One way of handling these radar dropouts was to use a weighted combination of the two radar readings when radar dropouts were suspected. Otherwise, only the EV300 radar range readings were used by the controller. The other two vehicles were also Buick LeSabre and they were equipped with data acquisition systems to record their speed and longitudinal acceleration.

For manual traffic, all vehicles were operated manually. The driver of the lead vehicle was instructed to follow a given speed profile to the best of his/her abilities. The drivers of the following vehicles responded by following the vehicle ahead with a comfortable headway. The vehicles were interchanged for different runs. Figure I-4 shows the experimental results for one such run.

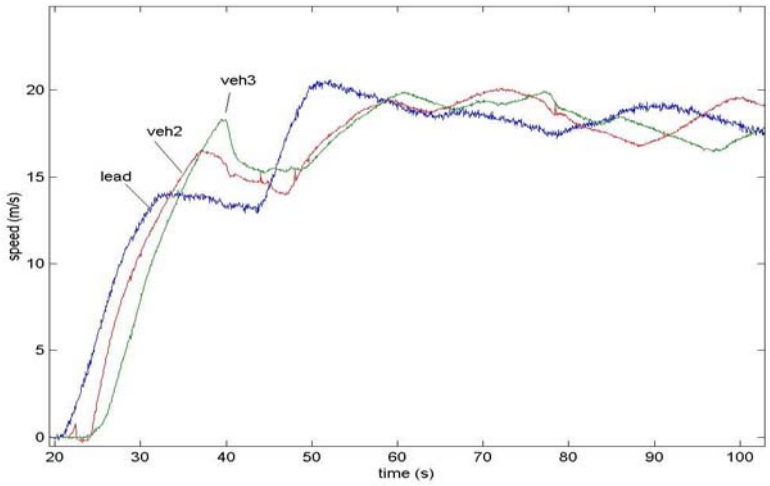

Figure I-4: Speed response of three manually driven vehicles during high acceleration maneuver: Experimental results

For mixed traffic experiments, the ACC algorithm was implemented on the Buick LeSabre that was used along with the two other Buicks. A time headway of 1.0 sec was used by the ACC vehicle. The lead vehicle performed as closely as possible the same type of maneuvers as in the manual traffic. The ACC vehicle was placed as the second vehicle for the vehicle following runs. Figure I-5 shows the responses of the three vehicles.

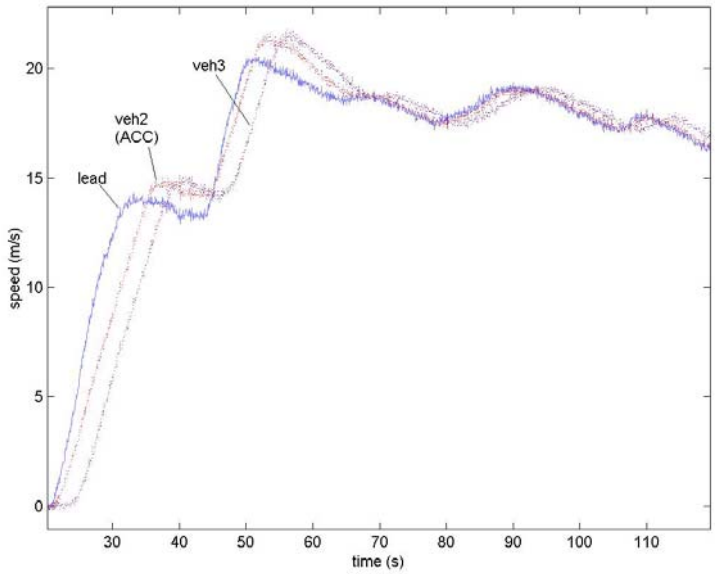

Figure I-5: Speed response in the mixed traffic during the high acceleration maneuver: 2nd vehicle is equipped with the ACC system. Experimental results.

Since the ACC vehicle is limited in maximum acceleration it lags behind, but its response and that of the 3rd vehicle is much smoother than that in Figure I-4 where all 3 vehicles were manually driven. Figure I-6 shows the speed responses of the 3 vehicles for lower lead vehicle acceleration. It is clear that the ACC vehicle is able to track closely the lead vehicle speed.

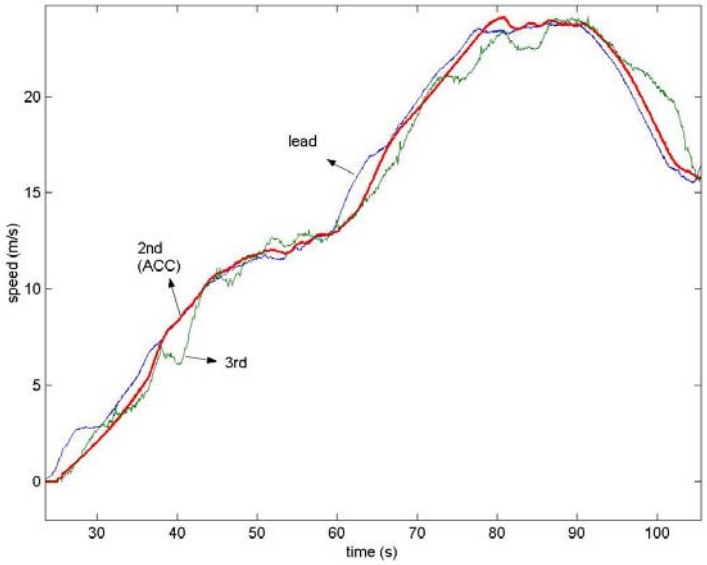

Figure I-6: Speed responses for a low acceleration lead vehicle maneuver. Experimental results

The speed responses in Figures I-4 and I-5 are fed into the emission model and the cumulative values of the emissions and fuel consumption were calculated. The percentage improvements caused by the presence of the ACC vehicle are calculated and summarized in Table 2. In order to validate the simulation results, obtained earlier and in the rest of the Chapter, the 3-vehicle experiment of Figures I-1 and I-2 is simulated using the mathematical models for the human drivers and the ACC system, and the benefits obtained are also presented in Table 2 for comparison purposes. It is clear that the simulations are more conservative in the estimate of the benefits than in the actual case. The same observation was made in [1].

Table 2. Summary of benefits

Benefits obtained in high acceleration maneuvers	Experimental results	Simulation results
CO emission benefits	12 %	6 %
HC emission benefits	6 %	5%
CO_2 emission benefits	Negligible	Negligible
NO_x emission benefits	7 %	6 %
Fuel consumption benefits	Negligible	Negligible

I-2.3 Sensitivity analysis

The results in [1] and in the previous section are obtained for a specific scenario that is likely to occur in an actual highway. The question that arises is how these benefits vary with respect to the 1) relative position of a (single) ACC vehicle in a string of manually driven vehicles; 2) acceleration and deceleration levels exhibited by the lead vehicle in the string, and 3) percent penetration of ACC vehicles in the mixed traffic.

I-2.3.1 Sensitivity analysis with respect to the position of a single ACC vehicle in a string of manually driven vehicles

We consider a string of 10 vehicles following the leader in a single lane. The lead vehicle performs high acceleration and deceleration maneuvers as shown in Figure I-1 (100% manual) and Figure I-2 (mixed). The only difference is that the ACC vehicle in the case of Figure I-2 is placed at different positions in the string of the 10 vehicles. In particular we consider a single ACC vehicle positioned 2nd, 4th, 6th and 8th place in the string. Environmental analyses for these three cases are carried out, and the percent improvements of mixed over manual traffic are calculated. Figure I-7 shows the variation of the benefits as the position of the ACC is moved away from the point where the traffic disturbance is generated. It is obvious that the further away the ACC vehicle is from the point of disturbance the less effect will have on the pollution levels and fuel economy of the vehicles in the string as the vehicles ahead of the ACC will perform as in the manual case. This indicates that the environmental benefits of ACC will improve with the penetration of ACC vehicles as more ACC vehicles are likely to be present close to the origin of the disturbance acting as filters of oscillatory high acceleration speed responses.

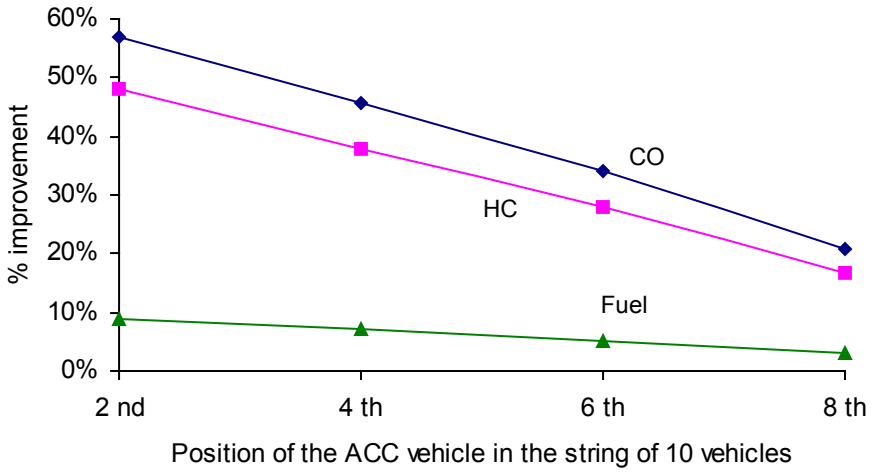

Figure I-7: Percent benefits in CO and HC emission and fuel consumption versus the position of the ACC vehicle in the string of 10 vehicles

In Figure I-7 the benefits in CO_2 and NO_x were less than 5% and considered to be negligible.

I-2.3.2 Sensitivity analysis with respect to the acceleration of the lead vehicle

In this subsection we examine the environmental impact of manual vs. mixed traffic with respect to the aggressiveness of the lead vehicle maneuver for a 10% ACC participation. As before we consider a string of 10 vehicles where the 3rd vehicle is ACC and the rest are manually driven. The lead vehicle starts from rest, accelerates at the specified rate (0.35g, 0.25g, 0.15g, 0.1g, 0.05g) to 24 m/s, and keeps that speed for ~100 sec. The rest follow suit. The speed responses in the manual and mixed case are used together with the emission model to calculate the cumulative percent benefits shown in Figure I-8.

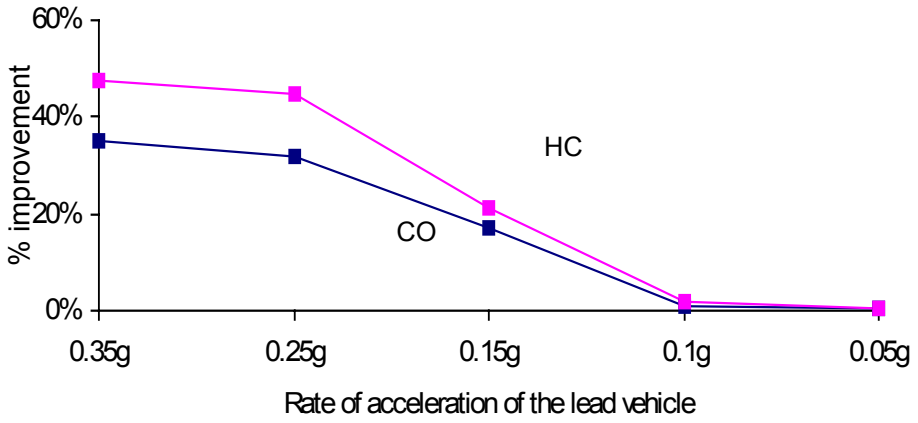

Figure I-8: Percent benefits in CO and HC emission vs. acceleration rate of lead vehicle maneuver

The benefits for NO_x, CO_2 and fuel consumption were less than 5% and considered to be negligible. As expected the benefits decreased with the level of the lead vehicle acceleration. Since the ACC vehicle is allowed to generate up to .1g acceleration the benefits for lead vehicle accelerations close to .1g and below are negligible. That is for accelerations close to .1g and below the ACC vehicle follows exactly the maneuver in an effort to maintain accurate position as in this case driver comfort is not an issue. As pointed out in [1] in this case the ACC vehicle simply passes the disturbance upstream with high accuracy without any filtering or attenuation.

I-2.3.3 Sensitivity analysis with respect to the penetration of ACC vehicles

Since the ACC vehicles act as filters of disturbances that are due to high acceleration maneuvers the more ACC vehicles are present in a string of vehicles the more effective this filtering effect will be. We study the case where 5%, 10%, 15% and 30% of the vehicles are ACC vehicles. In particular we consider a string of 20 vehicles where 5% corresponds to the presence of 1 ACC vehicle, 10% to 2 ACC vehicles , 15% to 3 ACC

vehicles and 30% to 6 ACC vehicles. The position of the ACC vehicles in the string of 20 is chosen randomly. Ten possible such positions are evaluated and the benefits obtained are averaged and presented in Figure I-9. The evaluation was performed for the following maneuver: The lead vehicle accelerates from 0 to 24 m/s with acceleration .35g and keeps that speed for a duration of about 100 sec and the rest of the vehicles follow accordingly. The results shown in Figure I-9 demonstrate that the benefits increase with a relatively small slope with the penetration of the ACC vehicles. As the penetration increases further the benefits level off. The results indicate that most of the benefits can be obtained even for low levels of penetration.

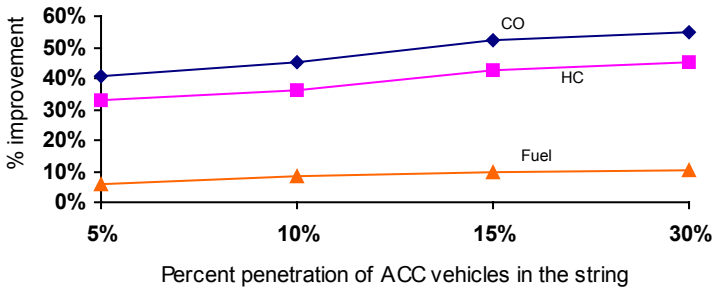

Figure I-9: Percent benefits in CO emission, HC emission and fuel consumption versus percent penetration of ACC vehicles

I-3 Lane Change Effects

As indicated before, the smooth response of the ACC vehicle may create large gaps in situations where the vehicle in front of the ACC vehicle speeds up with acceleration that is higher than the maximum allowed by the ACC system. One could argue that such large gaps may invite cut-ins from neighboring lanes, creating additional disturbances and negatively affecting the benefits established in [1] and in section I-2 above. Another one could also make the argument that advanced ACC systems may use smaller time headways during vehicle following which may discourage lane changes and therefore reduce disturbances due to lane changing. In this section, we examine the effect of cut-ins on the benefits reported in the previous section when during high acceleration maneuvers large gaps are created that invite a cut-in from the neighboring lane. Furthermore, we examine the effect of vehicles exiting the lane on the benefits established in section I-2. ACC vehicles may encourage such exits as with advanced forms of ACC where the time headway used may be small a driver may exit the lane in order to avoid being followed so close by a vehicle driven by a computer. In the following subsections we use simulations and experiments to evaluate the effects of cut-ins and exits.

I-3.1 Lane cut-ins: Simulations

Let us consider ten vehicles following each other in a single lane (lane 1), with the lead vehicle speeding with high acceleration. The increased inter-vehicle spacing between the ACC vehicle and the vehicle ahead invites a cut-in from the adjacent lane. For simplicity,

assume that only one vehicle from the neighboring lane (lane 2) performs a cut-in. The vehicles in lane 1 are traveling at steady state speed of 15 m/sec (33.5 mph) when the lead vehicle accelerates at 0.35g to reach a speed of 29 m/s (65 mph), and the rest follow suit. The ACC vehicle at the 4th position in lane 1 responds smoothly and lags behind the vehicle in front creating a large gap. The manually driven vehicle in lane 2 that was initially traveling at somewhat higher steady state speed of 16 m/sec (35.8 mph) takes advantage of the large gap in the neighboring lane to cut in between the ACC vehicle and the vehicle ahead.

Let us now the same situation with the ACC vehicle replaced with a manually driven one. In this 100% manual case we have two possible scenarios. In scenario 1 the vehicle behind the accelerating lead vehicle follows the lead vehicle equally aggressively leaving no space for the vehicle in lane 2 to cut in so no cut in takes place. This scenario is simulated in Figure I-10. In scenario 2 the vehicle behind the accelerating lead vehicle lags behind and the vehicle from the neighboring lane 2 manages to cut in. This scenario is shown in Figure I-11.

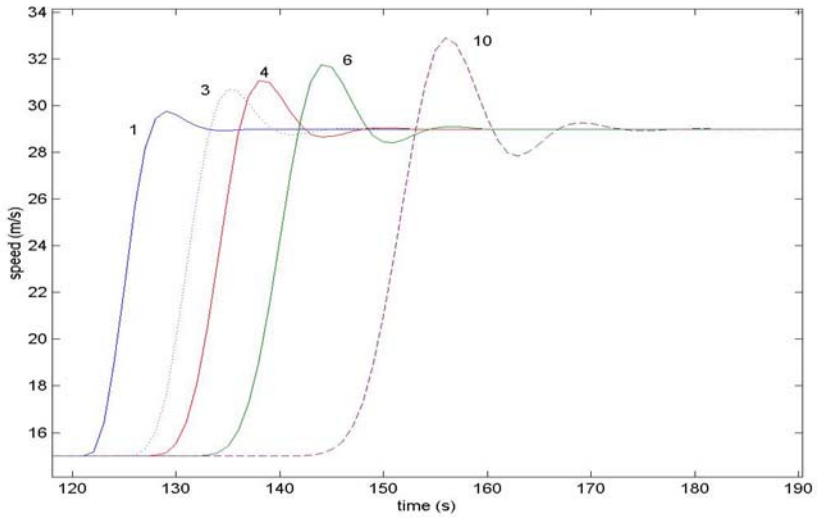

Figure I-10: (Manual case) Speed responses of the vehicles at positions 1, 3, 4, 6 and 10
(no cut-in)

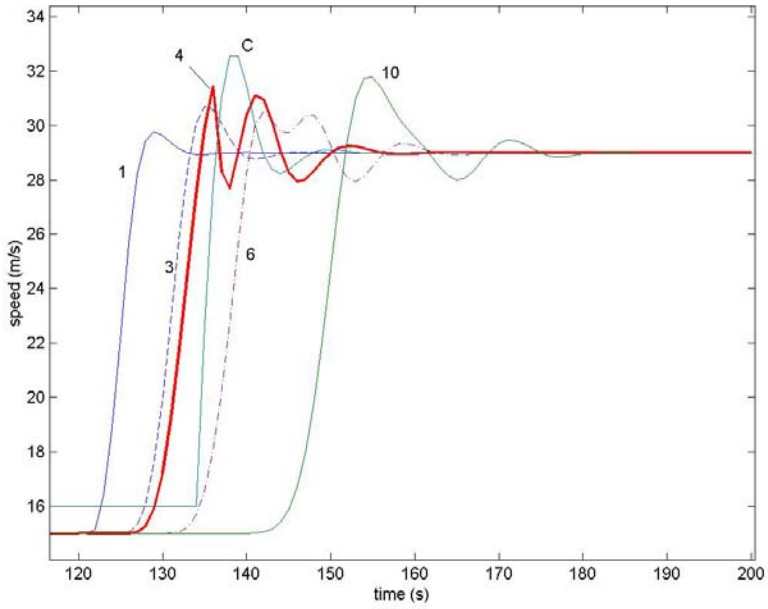

Figure I-11: (Manual case) Speed responses of the vehicles at positions 1, 3, 4, 6 and 10, as well as that of vehicle (C) from the adjacent lane and cuts-in in front of the 4th vehicle

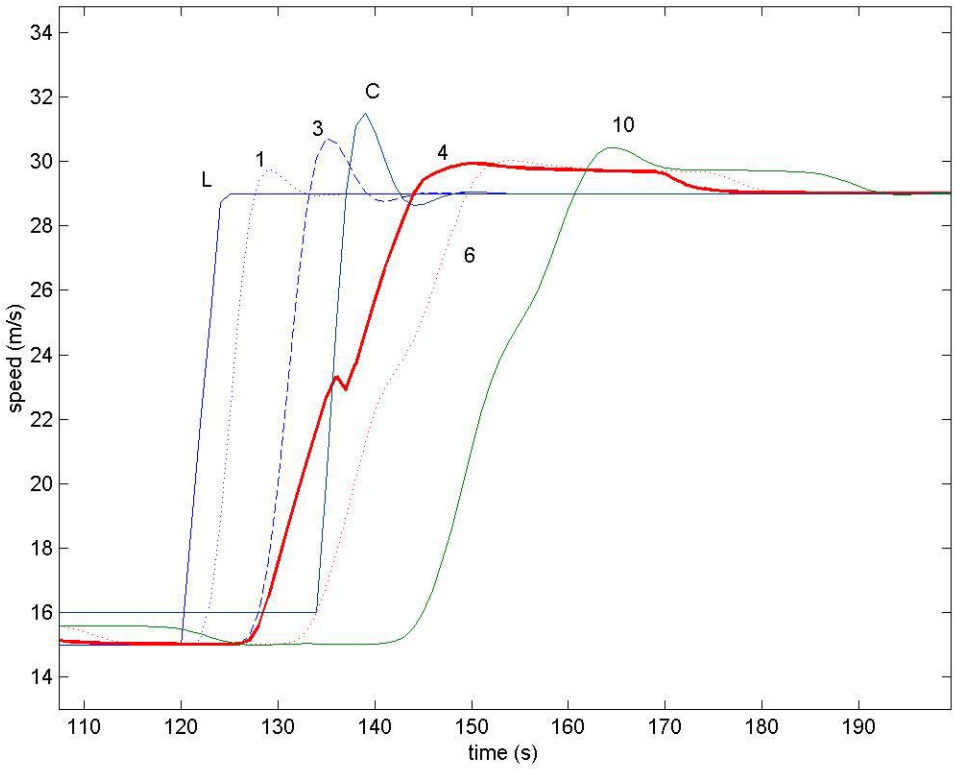

Figure I-12: Speed responses of the vehicles at position 1, 3, 4 (ACC), 6 and 10, as well as that of vehicle (C) from the adjacent lane that cuts-in in front of the ACC vehicle

Figure I-12 shows the speed responses of the mixed traffic in the cut-in situation: It is assumed that the neighboring lane vehicle cuts in immediately in front of the ACC vehicle, causing it to temporarily slow down, and then smoothly catch up with the new predecessor. Figure I-13 shows the position error of the ACC vehicle as it responds to the lead vehicle maneuver and switches targets from the lead to the cut-in vehicle.

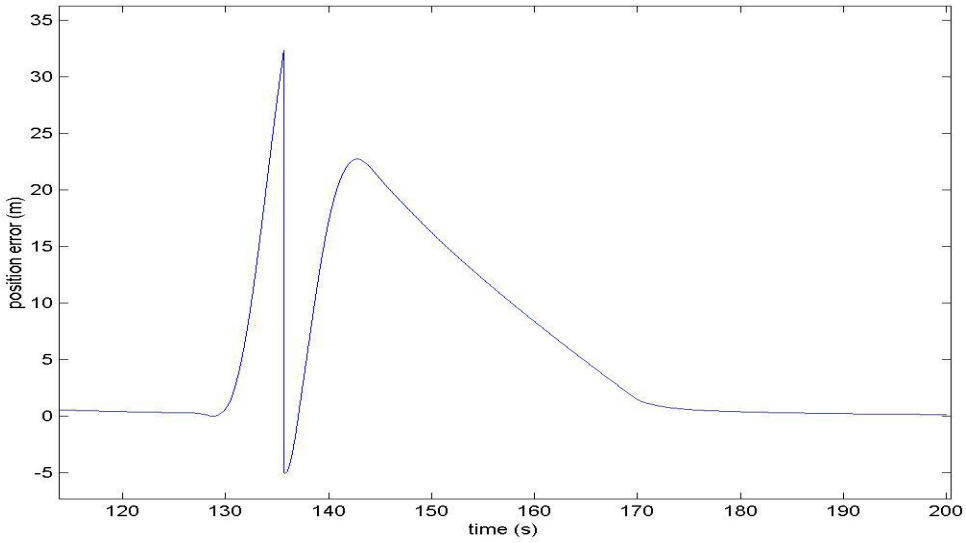

Figure I-13: Position error of the 4th (ACC) vehicle as it switches targets during the lane cut-in

Comparing the responses in Figures I-11 and I-12 it is clear that the presence of the ACC vehicle attenuates the disturbance due to the lead vehicle acceleration and cut-in vehicle effect.

The following Figures show similar results for a different lead vehicle acceleration maneuver. In this case, the lead vehicle in a string of 10 vehicles accelerates from 0 m/s to 20 m/s at 0.35g, keeps that speed for 140 sec, then decelerates to 11 m/s (~25 mph) at –0.25g, maintains that speed level for 50 sec, and finally accelerates at 0.3g to 26.8 m/s (60 mph). Figure I-14 shows the speed responses when all 10 vehicles are manually driven. The oscillatory response of the following vehicles and slinky effects are evident. Due to the tight vehicle following, it is assumed that no cut-in occurs by any vehicle from the adjacent lanes.

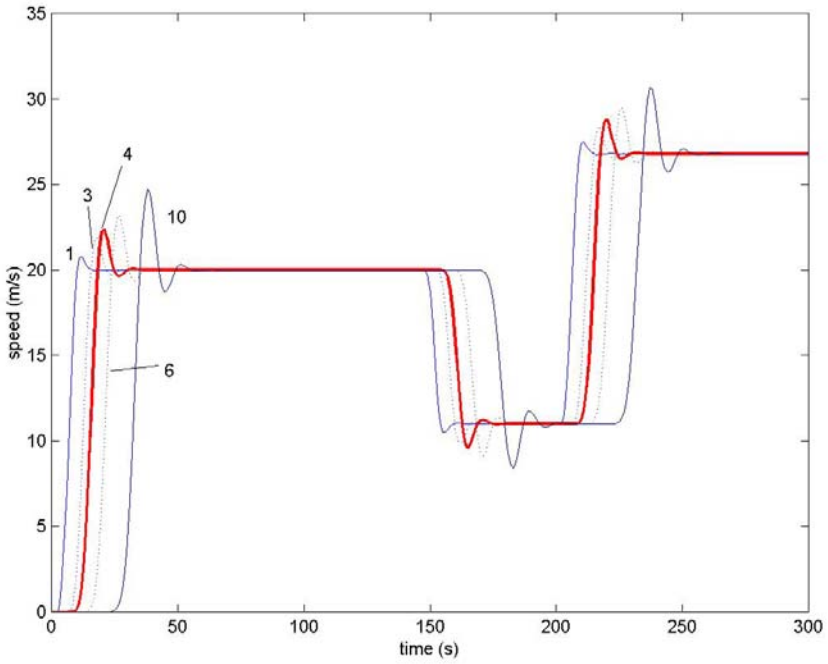

Figure I-14: Speed responses for 100% manual traffic

Figure I-15 shows the vehicle speed responses in the case where the 4th vehicle is an ACC vehicle. Due to the smooth response of the ACC vehicle, a large gap is created shown in the Figure I-16 that encourages a vehicle in the adjacent lane that is moving at the steady state speed of 15 m/s to cut in at t = 217 sec.

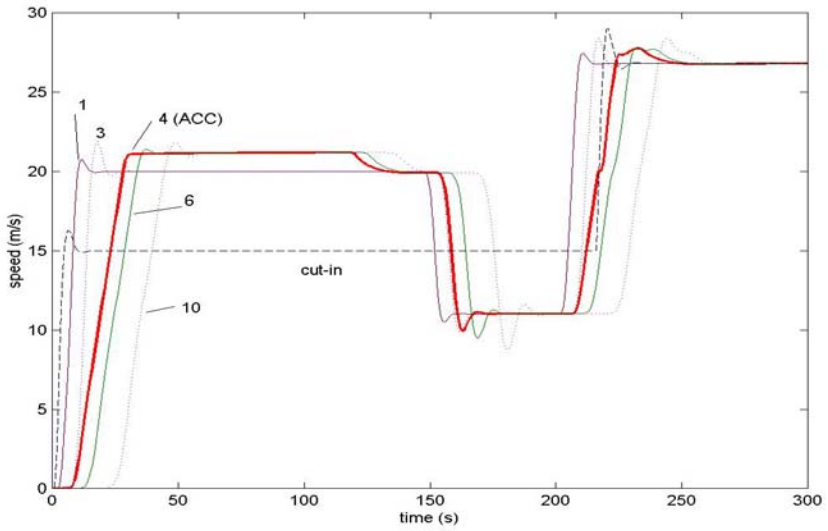

Figure I-15: Cut-in situation in mixed traffic: Speed responses of vehicles 1,3,4(ACC), 6, 10 and cutting-in vehicle C from adjacent lane versus time

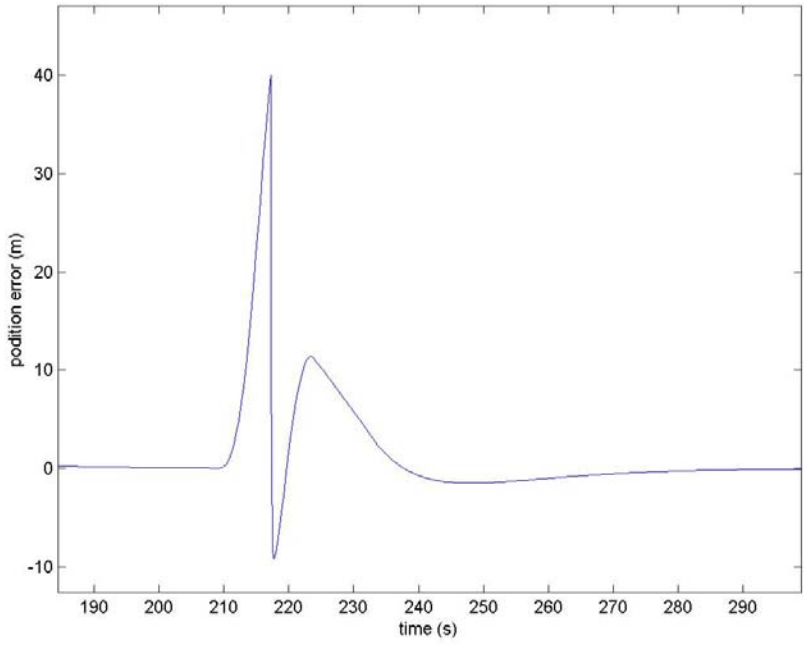

Figure I-16: Position error of the 4th (ACC) vehicle whose speed response is presented in Figure I-15

The above speed responses to the acceleration of the lead vehicle and cut-in vehicle disturbance are used with the emission model to calculate possible benefits that are due to the presence of the ACC vehicle in the string of vehicles in the following subsection.

I-3.2 Lane cut-ins: Environmental benefits

The speed responses in Figure I-10 to I-15 are used with the emissions model to calculate the percentage improvements obtained due to the presence of the ACC vehicle in the mixed over the manual traffic case. The results are summarized in Table 3:

Table 3: Summary of benefits

	Comparison of manual with a cut-in and mixed traffic (responses from Figure I-11 and I-12)	Comparison of manual with no cut-in and mixed traffic (responses from Figure I-10 and I-12)	Comparison of manual with no cut-in and mixed traffic (responses from Figure I-14 and I-15)
HC emission	23.8 %	24 %	30.2 %
CO emission	30.5 %	31 %	37.8 %
Fuel consumption	negligible	negligible	7.6 %

The results shown in Table 3 demonstrate that the cut-in invited by the ACC vehicle in a situation of high acceleration maneuvers that lead to large gaps will not take away the benefits calculated earlier in the absence of cut-ins.

The results in Table 3 are based on the assumption that the cut-in vehicle cuts in close to the ACC vehicle at about 7m causing the ACC vehicle to initially apply braking. The sensitivity of the results of Table 3 based on Figures I-11 and I-13 with respect to variations in the cut-in distance from the ACC vehicle are presented in Figure I-17.

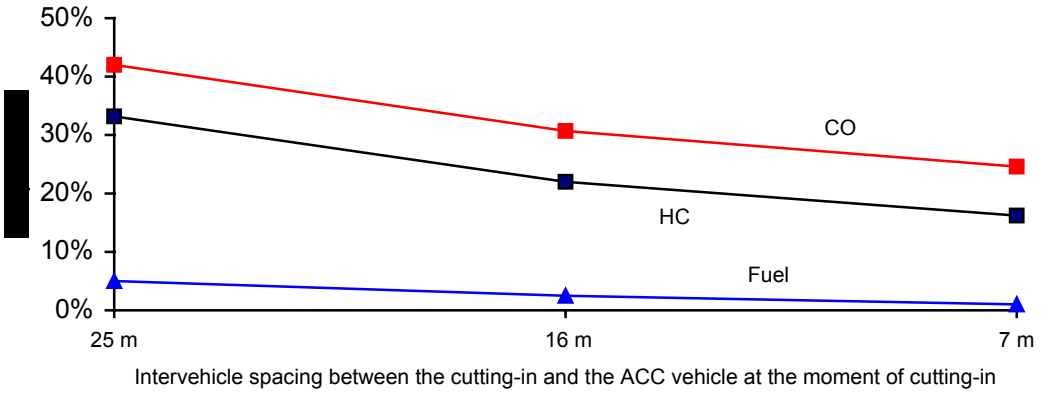

Figure I-17: Percent benefits in HC, CO emission and fuel consumption for lane cut-in situation in mixed traffic case vs. manual case without cut-ins, for three different cut-in distances between the neighboring-lane vehicle and the ACC vehicle

Results for the comparative emission of CO_2 and NO_x are not shown in Figure I-17 as they are negligible. What we observe from the obtained results above is that the benefits

in the lane cut-in situations depend largely on the spacing at which the manual vehicle cuts in front of the ACC one. In the case of a 'sharp' cut-in, i.e. when the initial cut-in spacing is only 7m, the ACC vehicle activates its brake actuator, which means additional disturbances in its response. When the distance is larger the level of braking is less and the disturbance due to the cut-in is smaller.

I-3.3 Lane cut-ins: Experiments

The behavior of the ACC vehicle during cut-in situations is tested at the testing facility at Crows Landing using one ACC vehicle and two manually driven vehicles. Several runs were conducted to evaluate the mixed traffic response during lane change situations. One of the typical runs that consisted of both lane change and lane exit, is shown in Figure I-18.

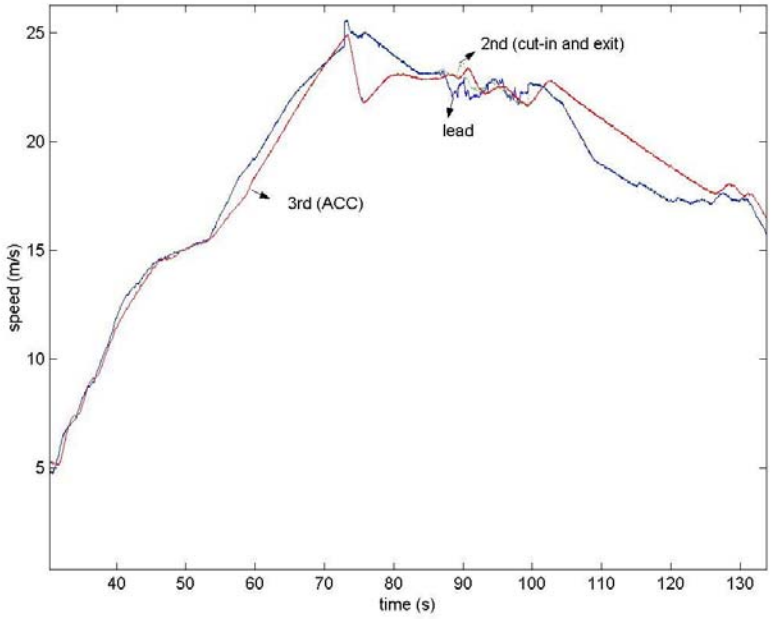

Figure I-18: Speed response of two manually driven and one ACC vehicle during the scenario that includes both lane exiting and cut-in maneuver.

As shown in Figure I-18, the lead manual vehicle accelerates from 0 m/s to 15 m/s, keeps that speed for a short while, then rapidly accelerates to ~25 m/s. The ACC vehicle follows by accelerating smoothly, thus increasing the inter-vehicle distance between the two vehicles. The 3rd experimental vehicle, traveling in the adjacent lane, cuts in between the two vehicles at approximately t = 73 sec. The ACC vehicle decelerates in order to maintain safe distance, then increases its speed to catch up with the target vehicle speed. At t = ~100s, the second vehicle leaves the lane, creating a large gap between the first and the third vehicle. Again, the ACC vehicle handles the disturbance in a smooth manner, eventually reducing the position error close to zero (see Figure I-19).

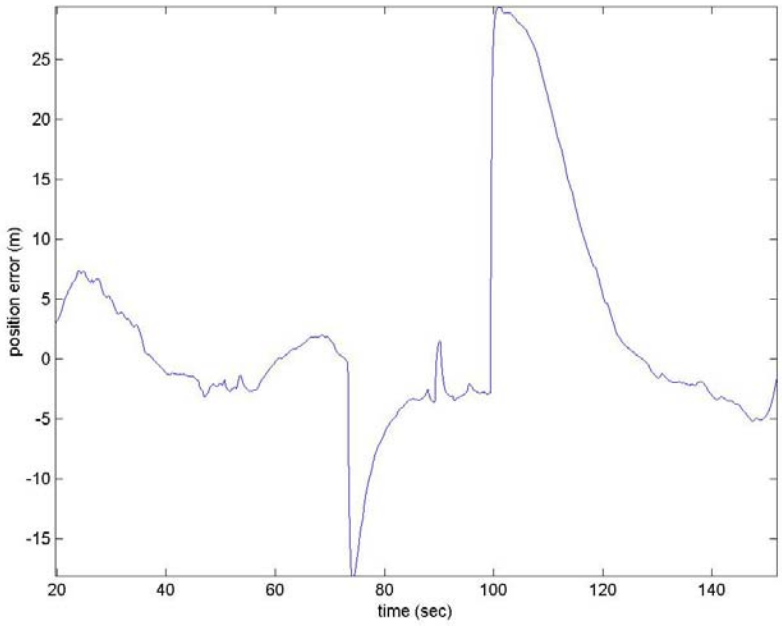

Figure I-19: Position error of the ACC vehicle during cut-in and exiting

The above experiment demonstrates experimentally the smooth response of the ACC vehicle to disturbances due to high acceleration maneuvers of the lead vehicle together with those due to cut-in and lane exit.

I-3.4 Lane exit: Simulations

Another type of abrupt traffic disturbance that may occur during vehicle following in a lane is due to a vehicle exiting the lane. This will create a gap that the vehicle behind will try to reduce by speeding up with all other vehicles in the string acting in a similar manner. In the case of a manual vehicle this could be done aggressively and in the case of an ACC vehicle the closing of the gap is done smoothly due to driver comfort and human factor constraints. We simulated and evaluated this scenario as follows:

We consider a string of 10 vehicles following a lead vehicle at steady state speed of 22.5 m/s (50 mph). At some point in time the 2nd vehicle exits the lane leaving a large gap between the 1st and 3rd vehicle. The 3rd manually driven vehicle that now becomes 2,nd speeds up to close the gap with an acceleration of about .15g. The vehicles behind follow suit trying to synchronize their speeds and maintain gaps that are comfortable for the individual drivers. We repeat the same experiment when the 3rd vehicle is an ACC that is designed to respond to such disturbance in a smooth manner. The results for the manual traffic case are shown in Figure I-20. The results for the mixed traffic case are shown in Figure I-21 with the corresponding position error shown in Figure I-22. It is clear from these Figures that the presence of the ACC vehicle reduced the effect of the disturbance considerably.

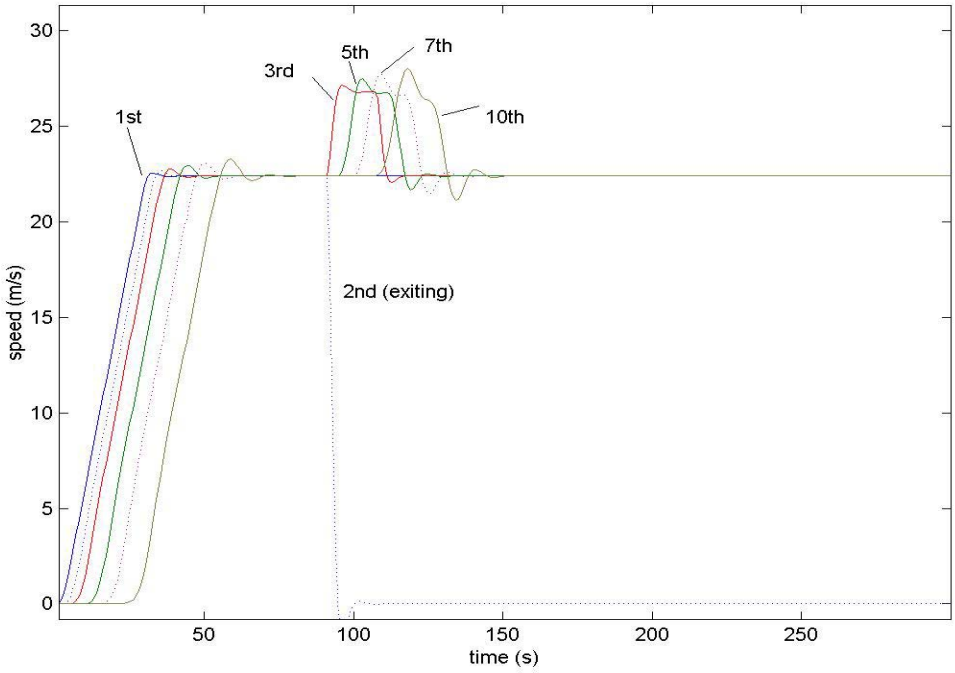

Figure I-20: Lane exit scenario, manual traffic. Speed responses of 1st, exiting 2nd, 3rd, 5th, 7th and 10th vehicles versus time.

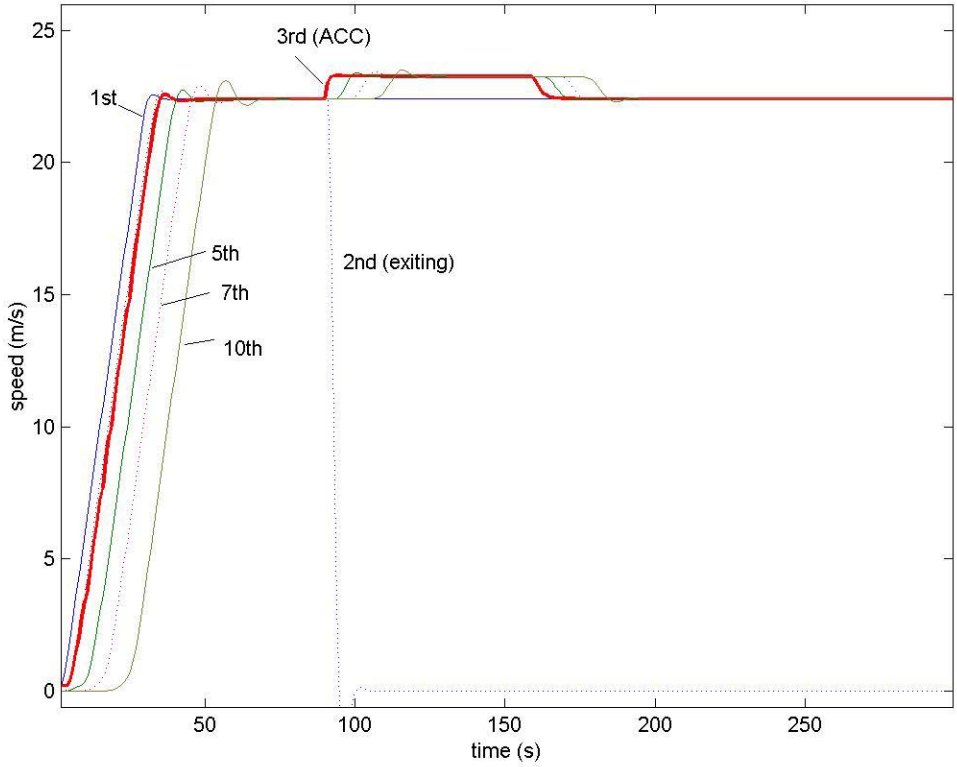

Figure I-21: Lane exit scenario, mixed traffic. Speed responses of 1st , exiting 2nd , 3rd (ACC), 5th, 7th and 10th vehicles versus time.

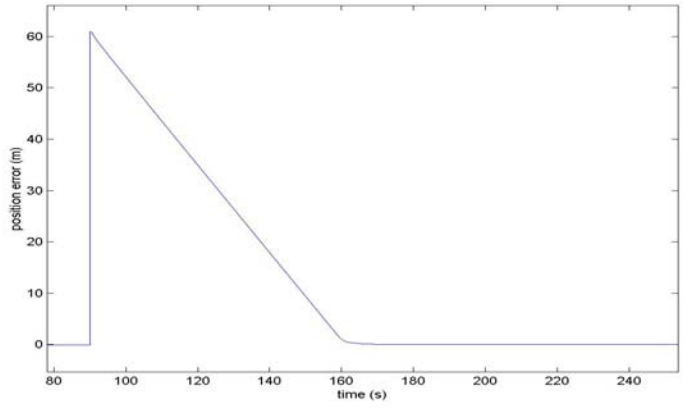

Figure I-22: Position error of the 3rd (ACC) vehicle versus time

In the following subsection we use the speed responses Figures I-20, I-21 and the emission model to calculate the effect of the ACC vehicle on the disturbance generated by the exit vehicle.

I-3.5 Lane exit: Environmental benefits

The following table shows the summarized benefits calculated for the mixed over manual traffic in the lane exit scenario described by Figures I-20, I-21 in Section I-3.4.

Table 4: Summary of benefits

	Percent benefits of mixed over manual traffic in lane exit scenario described by Figures I-20, I-21
HC emission	34 %
CO emission	49 %
CO_2 emission	5 %
NO_x emission	negligible
Fuel consumption	5 %

The results in Table 4 demonstrate that the presence of the ACC vehicle will reduce the effect of disturbances due to lane exit by the immediate vehicle ahead of the ACC in a way that is beneficial to the environment.

The results of Table 4 are obtained for the scenario described in Figures I-20, I-21 with the ACC vehicle located in the 3rd position (right behind the exit vehicle). We repeated the above scenario with the ACC vehicle located in the 4th, 6th and 9th position in the string of 10 vehicles while retaining the lane exit to take place at the 2nd vehicle position. The results are presented in Figure I-23.

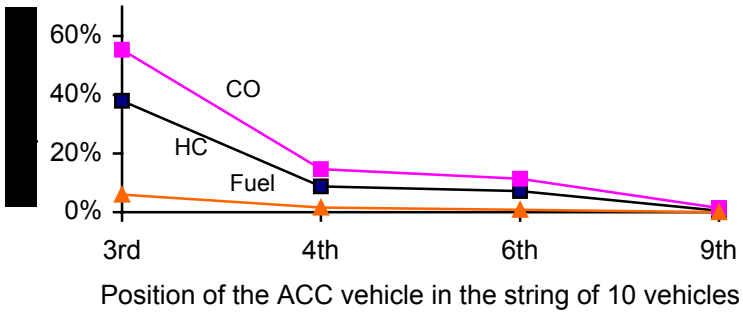

Figure I-23: Percent improvement in HC, CO emission and fuel consumption during a lane exit situation in mixed vs. manual traffic case where 2nd vehicle exits the lane versus the position of the ACC vehicle in the string of 10 vehicles

It is clear from Figure I-23 that the benefits in emission and fuel consumption are drastically reduced when the position of the ACC vehicle is shifted from the 3rd place (immediately behind the exit vehicle) to the 4th, 6th and 9th position. The reason is that the manual vehicles ahead of the ACC vehicle undergo speed response oscillations that do not correspond to high acceleration so that the ACC vehicle provides little attenuation. Instead it passes these oscillations on to the vehicles upstream. This simulation demonstrates that a higher penetration of ACC will lead to more benefits in terms of emissions and fuel economy in the presence of disturbances due to lane exit.

I-3.6 Lane exit: Experiments

The behavior of the ACC vehicle during the lane exit of the vehicle ahead is tested using actual vehicles at the test facility in Crows Landing. Three vehicles were used, two of them manually driven and one ACC. Figure I-24 shows one such run where the 2nd manually driven vehicle exits the string of the 3 vehicles at time t=81 sec. The following ACC vehicle switches targets and closes in smoothly. Figure I-25 shows the position error between the ACC vehicle and the vehicle in front. It increases almost instantaneously when the vehicle exits and the ACC vehicle switches targets but then it decreases smoothly to close to zero at steady state. The experimental results demonstrate the smoothness properties of the ACC vehicle during disturbances that arise because of vehicles exiting the lane which as analyzed in previous sections are responsible for the emissions and fuel economy benefits obtained when compared with the case where the ACC vehicle is replaced by a manually driven vehicle.

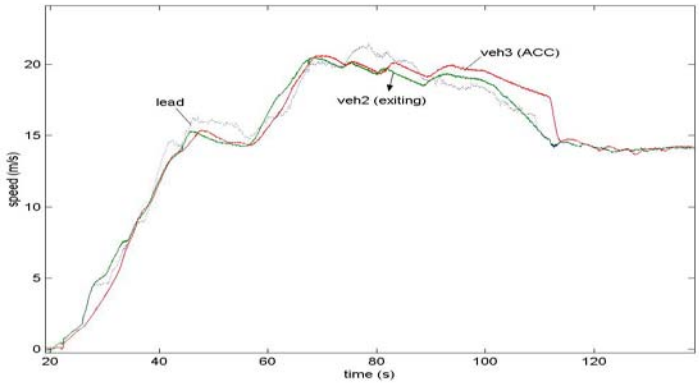

Figure I-24: Speed response of two manually driven and one ACC vehicle during lane exit maneuver. At ~81 sec, vehicle 2 exits the lane, and vehicle 3 (ACC) accelerates to catch up with the new predecessor

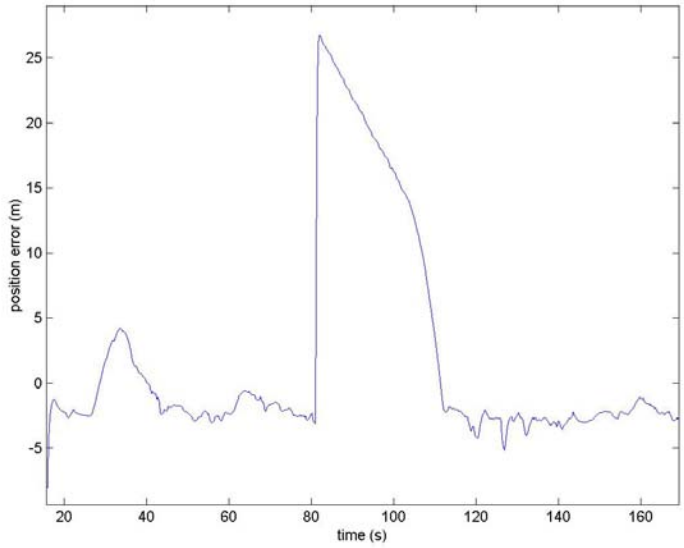

Figure I-25: Position error versus time of the ACC vehicle in lane exit scenario

4 Conclusion

In this Chapter we examined, using simulations and experiments, the mixed manual/ACC traffic characteristics on the microscopic level during disturbances that may arise due to high acceleration maneuvers and lane changes. The effect of the ACC vehicles is evaluated from the environmental point of view using an emissions model. We have demonstrated that the smooth response of the ACC vehicles has a beneficial effect on the environment in the presence of disturbances that are due to high acceleration maneuvers, lane cut –ins and lane exiting. These benefits vary with the levels of the disturbance, the position of the ACC vehicle in the string of manually driven vehicles and the ACC

vehicle penetration. Several sensitivity curves are developed that show the variation of the benefits with respect to the various variables.

Acknowledgments

We wish to thank the UCB/PATH experimental group for their assistance in collecting the data and valuable discussions during the experiments performed at the Crows Landing in July 2002.

References

[1] Bose, A. and Ioannou P., *Analysis of Traffic Flow with Mixed Manual and Intelligent Cruise Control Vehicles: Theory and Experiments*, California PATH Research Report UCB-ITS-PRR-2001-13

[2] Bose, A. and Ioannou, P., *Mixed Manual/Semi-Automated Traffic: A Macroscopic Analysis*, California PATH Research Report UCB-ITS-PRR 2001-14

[3] Bose, A. and Ioannou, P., *Analysis of Traffic Flow with Mixed Manual and Semi-Automated Vehicles*, California PATH Research Report UCB-ITS-PRR-99-14

[4] Pipes, L.A., *An Operational Analysis of Traffic Dynamics,* J. of Applied Physics, vol.24, pp.271-281, 1953.

[5] Barth, M.J., *Integrating a Modal Emissions Model into Various Transportation Modeling Frameworks*, ASCE Conference Proceedings, 1997.

[6] Barth, M.J. et al, *CMEM User's Guide*, UC Riverside, 2000.

[7] Ioannou, P. and Xu, T., *Throttle and Brake Control Systems for Automatic Vehicle Following*, IVHS Journal Vol. 1(4), pp. 345-377, 1994.

[8] Barth, M.J., *The Effect of AHS on the Environment*, in 'Automated Highway Systems', edited by P. Ioannou, Plenum Press, New York, 1997.

CHAPTER II

MIXED MANUAL/SEMI-AUTOMATED TRAFFIC: A MACROSCOPIC ANALYSIS

by
Arnab Bose and Petros Ioannou

Abstract

The use of advanced technologies and intelligence in vehicles and infrastructure could make the current highway transportation system much more efficient. Semi-automated vehicles with the capability of automatically following a vehicle in front as long as it is in the same lane and in the vicinity of the forward looking ranging sensor are expected to be deployed in the near future. Their penetration into the current manual traffic will give rise to mixed manual/semi-automated traffic. In this Chapter, we analyze the fundamental flow-density curve for mixed traffic using flow-density curves for 100% manual and 100% semi-automated traffic. Assuming that semi-automated vehicles use a time headway smaller than today's manual traffic average due to the use of sensors and actuators, we have shown using the flow-density diagram that the traffic flow rate will increase in mixed traffic. We have also shown that the flow-density curve for mixed traffic is restricted between the flow-density curves for 100% manual and 100% semi-automated traffic. We have presented in a graphical way that the presence of semi-automated vehicles in mixed traffic propagates a shock wave faster than in manual traffic. We have demonstrated that the presence of semi-automated vehicles does not change the total travel time of vehicles in mixed traffic. Though we observed that with 50% semi-automated vehicles a vehicle travels 10.6% more distance than a vehicle in manual traffic for the same time horizon and starting at approximately the same position, this increase is marginal and is within the modeling error. Lastly, we have shown that when shock waves on the highway produce stop-and-go traffic, the average delay experienced by vehicles at standstill is lower in mixed traffic than in manual traffic, while the average number of vehicles at standstill remains unchanged.

II-1 Introduction

During the past decade, researchers have focussed on improving traffic flow conditions with the help of automation. Several concepts that have been proposed include automation in the driver-vehicle system or the infrastructure or both. While fully automated vehicles on dedicated highways are seen as a far in the future objective, the use of partial or semi-automated vehicles on current highways with manually driven vehicles is deemed as a near-term goal.

Semi-automated vehicles are those that have the capability of automatically following a vehicle in front as long as it is in the same lane and within the range of the forward looking ranging sensor [6]. The vehicles use a longitudinal controller such as the Intelligent Cruise Control (ICC) system that comprises of throttle and brake subsystems [3]. The external input variables used by the ICC vehicle are the relative speed and the

relative distance between itself and the leading vehicle (if any), in addition to its own speed obtained using different sensors [9].

The use of sensors and actuators makes it possible for semi-automated vehicles to have a lower reaction time than manually driven vehicles. As a result, a semi-automated vehicle uses a smaller time headway and intervehicle spacing than current manual traffic average and reacts almost instantaneously to a speed differential in comparison to a manual vehicle. Intervehicle spacing is the distance between the same points in successive vehicles. Time headway is the time taken to cover the distance between the rear of the front vehicle to the front of the following vehicle. Human factor considerations demand that the response of an ICC vehicle be smooth for passenger comfort. Hence a semi-automated vehicle acts as a filter that smoothes out traffic flow disturbances [12]. The principle question is what will be the effect of the gradual penetration of semi-automated vehicles among manual ones on the mixed traffic flow, especially during the presence of disturbances.

In this Chapter we focus our attention to the macroscopic analysis of mixed traffic flow. Two topics addressed are fundamental flow-density diagrams and shock waves. A fundamental flow-density diagram defines the steady-state relation between the traffic flow rate and the traffic density [1]. It is dependent on factors under which the traffic flow rate and the traffic density are observed like the length of time interval over which data is aggregated [11]. We outline flow-density diagrams for 100% manual and 100% semi-automated traffic. A linear follow-the-leader human driver model is used to model the dynamics of manually driven vehicles [2,7,11,16]. The model assumes that the human driver observes only the vehicle in front and sets its vehicle acceleration depending on the relative speed and the relative distance. A manual traffic flow-density curve is constructed using this human driver model. It has a stationary point that corresponds to maximum manual traffic flow rate. A flow-density curve for 100% semi-automated vehicles is constructed using the ICC design given in [3]. The highest point of the curve corresponds to maximum semi-automated traffic flow rate. We show using these flow-density curves that for any given traffic density, mixed traffic flow rate is greater than manual traffic flow rate. We also show that the mixed traffic flow-density curve is restricted in the region encapsulated by these curves. As the percentage of semi-automated vehicles increases, this curve converges to the flow-density curve for 100% semi-automated traffic.

The effect of semi-automated vehicles among manual ones during the presence of traffic flow disturbances such as shock waves is shown using space-time diagrams and demonstrated using simulations. Shock waves are discontinuous waves that occur when traffic on a section of a road is denser in front and less dense behind. We present in a graphical way that the presence of semi-automated vehicles in mixed traffic propagates a shock wave faster than in manual traffic. We demonstrate that a vehicle in mixed traffic with 50% semi-automated vehicles travels 10.6% more distance than a vehicle in manual traffic for the same time horizon and starting at approximately the same position. A linear follow-the-leader human driver model, namely Pipes model [7,8] has been validated to closely model current manual driving [20]. Hence it is used to model the dynamics of

manual vehicles during the simulations. A three-dimensional representation of space-time diagrams is used to show that the traffic flow rate and the traffic density in mixed traffic are greater than that in manual traffic.

Lastly, we show that when shock waves produce stop-and-go traffic on the highway, the average delay experienced by vehicles is lower in mixed traffic than in manual traffic, while the average number of vehicles at standstill remains unchanged.

This Chapter is organized as follows: Section II-2 introduces the traffic flow variables and analyzes mixed traffic flow using flow-density diagrams for 100% manual, 100% semi-automated and mixed traffic. Section II-3 deals with shock waves and the effect of semi-automated vehicles on them. Section II-4 compares the average delay experienced by vehicles during stop-and-go conditions on the highway in manual and mixed traffic. A summary of the main results is provided in the concluding Section II-5.

II-2 Fundamental Flow-Density Diagram

Traffic flow rate q and traffic density k are average measures of traffic flow characteristics. The precise definition of q and k and the means of measuring them are explained in [1]. In this Section we consider the flow-density diagrams for 100% manual traffic, 100% semi-automated traffic and analyze the flow-density curve for mixed manual/semi-automated traffic. A fundamental flow-density diagram defines the steady-state relation between the traffic flow rate and the traffic density [1]. It is dependent on factors under which the traffic flow rate and the traffic density are observed like the length of time interval over which data is aggregated [11].

II-2.1 Manual Traffic

A linear car-following model is used to model the motion of a manual vehicle. The car-following theory assumes that traffic stream is a superposition of vehicle pairs where each vehicle follows the vehicle ahead according to some specific stimulus-response equation [2,7,16]. Using Fig. II-1 we have the acceleration of the $(n+1)^{th}$ vehicle given by [11]

$$\ddot{x}_{n+1}(t+\tau) = \lambda[\dot{x}_n(t) - \dot{x}_{n+1}(t)] \qquad (1)$$

where

τ : reaction time lag

λ : sensitivity factor and $\lambda = \lambda_0 \dfrac{\dot{x}^m{}_{n+1}(t+\tau)}{[x_n(t) - x_{n+1}(t)]^l}$

This is referred to as the (m, l) model. For m=0, l=1.5 we obtain

$$\ddot{x}_{n+1}(t+\tau) = \lambda_0 \frac{[\dot{x}_n(t) - \dot{x}_{n+1}(t)]}{[x_n(t) - x_{n+1}(t)]^{1.5}}$$

or,

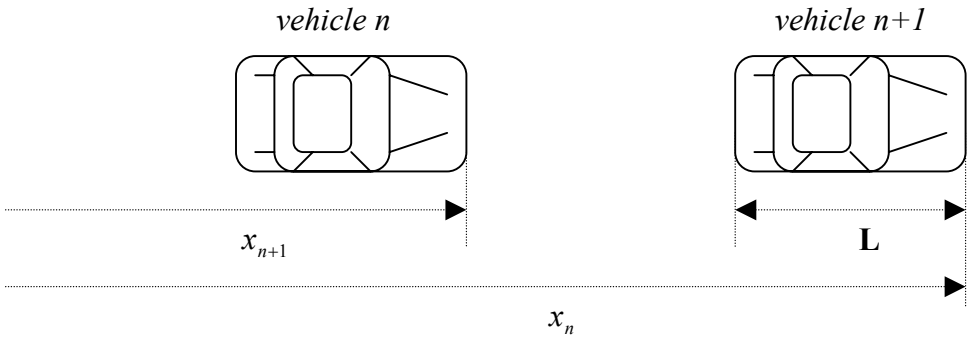

Figure II-1: Vehicle following in a single lane.

$$\dot{v}_{n+1}(t+\tau) = \lambda_0 \frac{\dot{s}_{n+1}}{s_{n+1}^{1.5}}, \tag{2}$$

where v_{n+1} : speed of $(n+1)$-th vehicle
$s_{n+1} = x_n(t) - x_{n+1}(t)$: intervehicle spacing of the $(n+1)$-th vehicle

The intervehicle spacing is defined as the distance between same points in successive vehicles.

To analyze the macroscopic effect we neglect the reaction time lag τ. In [11] it is shown that the time lag does not affect the equation that describes the macroscopic traffic flow behavior. Dropping the subscripts in (2) we get

$$\dot{v} = \lambda_0 \frac{\dot{s}}{s^{1.5}} \tag{3}$$

It can be shown that the reciprocal of the average intervehicle spacing is the traffic density [4]. Therefore, using $k = \frac{1}{s}$ where k represents the traffic density, we can express (3) as

$$\dot{v} = -\lambda_0 k^{1.5} \frac{\dot{k}}{k^2} \tag{4}$$

Integrating (4) we have

$$\int_{v}^{0} \dot{v} = -\lambda_0 \int_{k}^{k_j} \frac{\dot{k}}{k^{0.5}} \tag{5}$$

where the limits are from the present point (v,k) to the jam condition where all vehicles are at standstill, i.e. $v = 0$ and $k = k_j$, where k_j is the traffic density at jam condition. Evaluating (5) we get

$$v = 2\lambda_0\left(\sqrt{k_j} - \sqrt{k}\right) \tag{6}$$

The proportionality constant λ_0 in (6) can be expressed in terms of speed and traffic density using $v = v_f$ when $k = 0$, i.e. when the density is negligible, there is no vehicle-to-vehicle interaction and vehicles travel at mean free speed v_f. The mean free speed is the vehicle speed that is not affected by other vehicles and only subjected to constraints associated with the vehicle and road characteristics. That gives us

$$\lambda_0 = \frac{v_f}{2\sqrt{k_j}}$$

Substituting for λ_0 in (6) we obtain the average speed of vehicles on a section of the road

$$v = v_f\left(1 - \sqrt{\frac{k}{k_j}}\right) \tag{7}$$

where

v_f : mean free speed that corresponds to negligible traffic density when there is no interaction among vehicles.

k : traffic density on the section of the road.

k_j : jam density equal to $1/L$ where L is the average length of vehicles, i.e. the traffic density corresponding to jam conditions when the vehicles are stacked bumper-to-bumper and the speed is zero.

The traffic flow rate q at steady state measures the number of vehicles moving in a specified direction on the road per unit time and is given by

$$q = kv \tag{8}$$

Substituting v from (7) we get an equation of the manual traffic flow-density relationship at steady state given by

$$q = kv = kv_f\left(1 - \sqrt{\frac{k}{k_j}}\right) \equiv Q(k) \tag{9}$$

which is also used to obtain the fundamental $q-k$ diagram shown in Fig. II-2.

The speed of waves carrying continuous changes of flow along the vehicle stream is the slope of the tangent to the $q-k$ curve at a point and is given by

$$c = \frac{dq}{dk} = \frac{d(kv)}{dk} = v + k\frac{dv}{dk} \tag{10}$$

The wave speed is smaller than the average speed of the vehicles when the latter decreases with increase in traffic density, i.e. $\frac{dv}{dk} \leq 0$. The equality holds when the density is very low and any increase does not affect the average speed of the vehicles. Such conditions exist in the vicinity of the origin of the $q-k$ diagram where the density is negligible and there is no vehicle-to-vehicle interaction.

The $q-k$ curve has a stationary point that corresponds to a critical density k_{cm} that gives the maximum traffic flow rate q_{mm} or the capacity on the section of the road. The slope of the line joining a point on the $q-k$ curve to the origin gives the average speed of vehicles at that point. The equation (9) is an example of a flow-density model derived from the (*m,l*) model and is used to qualitatively describe manual traffic flow characteristics. Different values of *m* and *l* are used to obtain a good fit to actual traffic flow data. For example, in [1] it is mentioned that the flow-density model derived with *m*=0.8 and *l*=2.8 gives a good fit to data observed on an expressway in Chicago. The flow-density model derived using *m*=1 and *l*=3 is shown to be qualitatively valid for traffic flow characteristics observed in 3-lane Boulevard P9riph9rique de Paris [16]. Likewise, *m*=0 and *l*=1 is used to derive a flow-density model that gives a good fit to actual traffic flow data taken in the Lincoln Tunnel in New York [17].

The point (q_{mm}, k_{cm}) has been empirically observed to be unstable, i.e. it leads to a breakdown in traffic flow. When traffic flow conditions exist at or near this point, the traffic flow and the average speed decreases as traffic density increases, and the operating point moves towards the jam density k_j on the $q-k$ curve. This observation is explained in [15]. As capacity is approached, flow tends to become unstable as the number of available gaps reduces. Traffic flow at capacity means that there are no usable gaps left. A disturbance in such a condition due to lane changing or vehicle merging is not 'effectively damped' or 'dissipated'. This leads to a breakdown in traffic flow and 'formation of upstream queues'. As pointed in [15], this is the reason why all facilities are designed to operate at lower than maximum traffic flow conditions.

II-2.2 Semi-Automated Traffic

While the behavior of human drivers is random and at best we can develop a manual traffic flow-density model that is qualitatively valid, the responses of semi-automated

vehicles are deterministic due to the use of computerized longitudinal controllers. In this Section, we utilize this advantage along with certain assumptions to develop a deterministic semi-automated traffic flow-density model that is used to obtain the fundamental $q - k$ diagram.

A semi-automated vehicle uses a longitudinal controller to automatically follow a vehicle in the same lane and within the range of its forward looking ranging sensor. Many such controller designs exist in literature that use constant time headway [3,14] and constant spacing [13] policies. In this Chapter we consider the ICC design given in [3] which uses a constant time headway policy. The time headway is defined as the time taken to travel the distance between the rear end of the lead vehicle and the front end of the following vehicle.

.

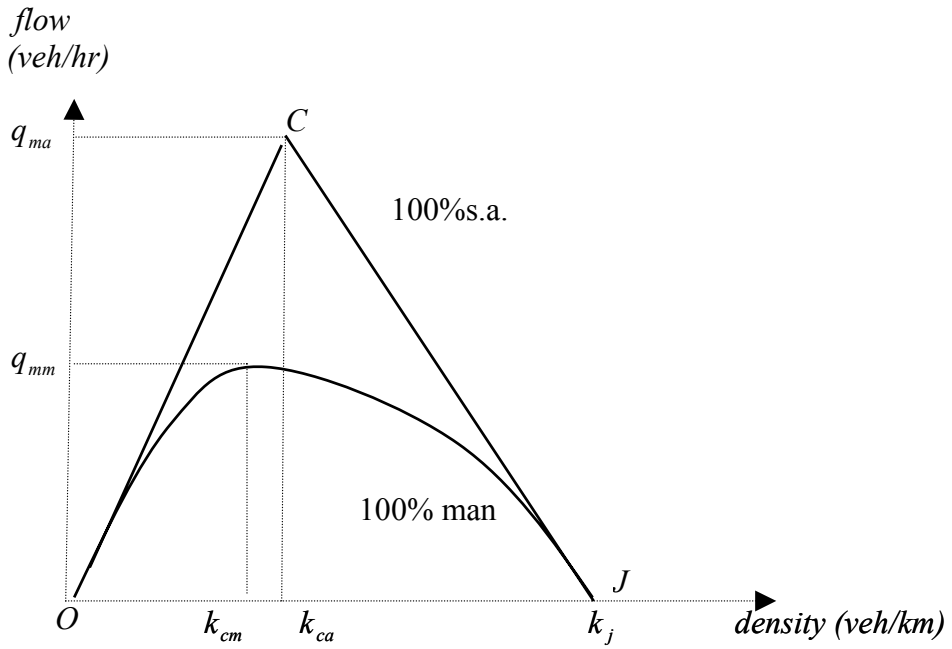

Figure II-2: Fundamental flow-density curves for 100% manual traffic and 100% semi-automated traffic.

The intervehicle spacing s at a speed v followed by a semi-automated vehicle using a constant time headway h_a is given by

$$s = h_a v + L \tag{11}$$

where L is the length of the vehicle. For simplicity we assume that all semi-automated vehicles have the same length L and use the same time headway h_a.

The average intervehicle spacing is the reciprocal of traffic density. When traffic density is such that the intervehicle spacing is greater than or equal to that given by (11), then during this period at steady state the traffic flow rate given by (8) increases linearly with the density of semi-automated vehicles according to

$$q = kv_f$$

where v_f is the mean free speed. This situation is indicated by the line *OC* in Fig. II-2.

As the traffic density increases and reaches the value

$$k = k_{ca} = \frac{1}{h_a v_f + L}$$

the maximum semi-automated traffic flow rate q_{ma} or capacity is reached. Thereafter, the relation between q and k can no longer change unless the speed v_f or the time headway h_a changes. It is reasonable to assume that the time headway h_a is fixed at all speeds and further increase in k occurs due to changes in speed. In such a case we have

$$s = h_a v + L < h_a v_f + L \tag{12}$$

and

$$k = \frac{1}{h_a v + L} > k_{ca} = \frac{1}{h_a v_f + L} \tag{13}$$

Thus, the speed of the semi-automated vehicles decreases with increasing k according to

$$v = \frac{1}{h_a}\left(\frac{1}{k} - L\right) \tag{14}$$

The traffic flow rate is given by

$$q = kv = \frac{1}{h_a}(1 - kL)$$

Graphically, the slope of the line joining the origin to a point on the $q - k$ curve gives the speed of the semi-automated vehicles at that point. It can be seen that before the critical density the speed remains constant at v_f. After reaching the critical density k_{ca}, the speed falls as the traffic density increases (Fig. II-2).

Therefore the steady state fundamental flow-density diagram for 100% semi-automated traffic is given by

$$q = \begin{cases} kv_f & k \le k_{ca} \\ \dfrac{1}{h_a}(1 - kL) & k > k_{ca} \end{cases} \tag{15}$$

Equation (15) describes the average steady state traffic flow characteristics. They do not capture any effects due to individual vehicle responses.

In region *OC* of the $q - k$ curve, the critical density is not yet reached. The average speed of the semi-automated vehicles is equal to the mean free speed v_f. This region corresponds to "loose" vehicle following where some semi-automated vehicles travel without following any vehicle and use an intervehicle spacing greater than that given by (11). The rest follow a lead vehicle and use an intervehicle spacing given by (11). After *C* the average speed of the semi-automated vehicles along with the traffic flow rate begin to decrease with increase in density. This region indicated by the line *CJ* corresponds to "tight" vehicle following where all semi-automated vehicles follow a lead vehicle and use an intervehicle spacing given by (12). Finally, at maximum density k_j all semi-automated vehicles are at dead stop and stacked bumper-to-bumper.

Let us now consider the stability of the point (q_{ma}, k_{ca}). We mentioned in the previous subsection that the corresponding point (q_{mm}, k_{cm}) in manual traffic has been empirically observed to be unstable. Obviously, it is not possible to empirically determine the stability of (q_{ma}, k_{ca}). However, it is expected that the point (q_{ma}, k_{ca}) will also be unstable, i.e. at this operating point there will be a breakdown in traffic flow. As in manual traffic, flow will tend to become unstable as capacity is approached and the number of available gaps reduces. At critical density there will be no usable gaps left. Any disturbance generated at this condition is expected to lead to the formation of upstream queues and a breakdown in traffic flow, as observed in manual traffic. Furthermore, it has been shown that traffic flow in the region *CJ* where the intervehicle spacing is given by (13) is unstable in the sense that disturbances propagate upstream unattenuated [21].

II-2.3 Mixed Manual/Semi-Automated Traffic

In the previous subsections, at one end we developed a flow-density model that qualitatively describes manual traffic flow characteristics. At the other end, we developed a deterministic flow-density model for semi-automated traffic. A combination of these two models is expected to characterize mixed manual/semi-automated traffic flow, which we analyze in this Section. We assume that at steady state conditions vehicles of the same class use identical headways and intervehicle spacings. For semi-automated vehicles this is equal to the designed value of the ICC controller. For manual vehicles, we take it to be equal to the average value observed in current manual traffic.

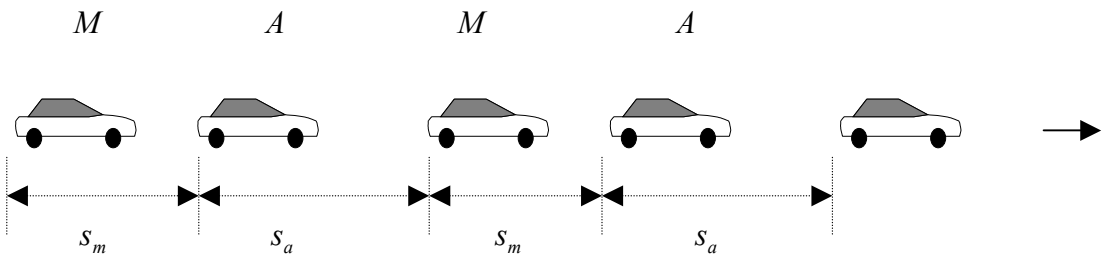

Figure II-3: Mixed manual/semi-automated traffic.

Consider the mixed traffic flow shown in Fig. II-3. Manual vehicles are marked '*M*' and semi-automated vehicles are marked '*A*'. Assuming moderately dense traffic conditions, the average intervehicle spacing at steady state conditions is given by

$$\bar{s} = ps_a + (1-p)s_m \tag{16}$$

where

p: market penetration of semi-automated vehicles in mixed traffic.

$s_a = h_a v + L$: intervehicle spacing used by semi-automated vehicles at speed v with time headway h_a; L is the average length of the vehicle.

$s_m = h_m v + L$: average intervehicle spacing used by manual vehicles at speed v for a time headway h_m which is the average of current manual traffic time headway distribution.

Remark 1: Throughout this Chapter, we assume that due to the use of sensors and actuators in semi-automated vehicles, $h_a < h_m$, i.e. $s_a < s_m$ at a given speed and for the same average length of manual and semi-automated vehicles [6].

The total mixed traffic density is given by

$$k_{mix} = \frac{1}{\bar{s}} \equiv f(p, s_a, s_m) \tag{17}$$

We assume that the driver of a manual vehicle behaves the same way whether following a semi-automated vehicle or a manual vehicle. Under this assumption, we can use the fundamental flow-density curve for 100% manual traffic to determine the characteristics of manual vehicles in mixed traffic. Likewise, the flow-density curve for 100% semi-automated traffic can be used for semi-automated vehicles in mixed traffic, as their vehicle dynamics remain unchanged when following a manually driven vehicle.

The steady state speed of mixed traffic is determined by the speed of the slowest moving vehicle class (manual or semi-automated). Using the above assumption, we take the

inverse of the average intervehicle spacing for each vehicle class as their density, i.e. $k_m = \frac{1}{s_m}$ and $k_a = \frac{1}{s_a}$. Then use (7) and (14) to determine the average speeds at which the manual and the semi-automated vehicles can travel. The lower of the two determines the speed at which all vehicles travel in mixed traffic. Note that from (17) the density of each class is dependent on the other.

Lemma 1: The $q-k$ curve for mixed manual/semi-automated traffic remains in the region between the $q-k$ curves for 100% manual and 100% semi-automated traffic. Furthermore, the mixed traffic flow rate is greater than the manual traffic flow rate for the same traffic density.

Proof:

Case 1: $v_a > v_m$

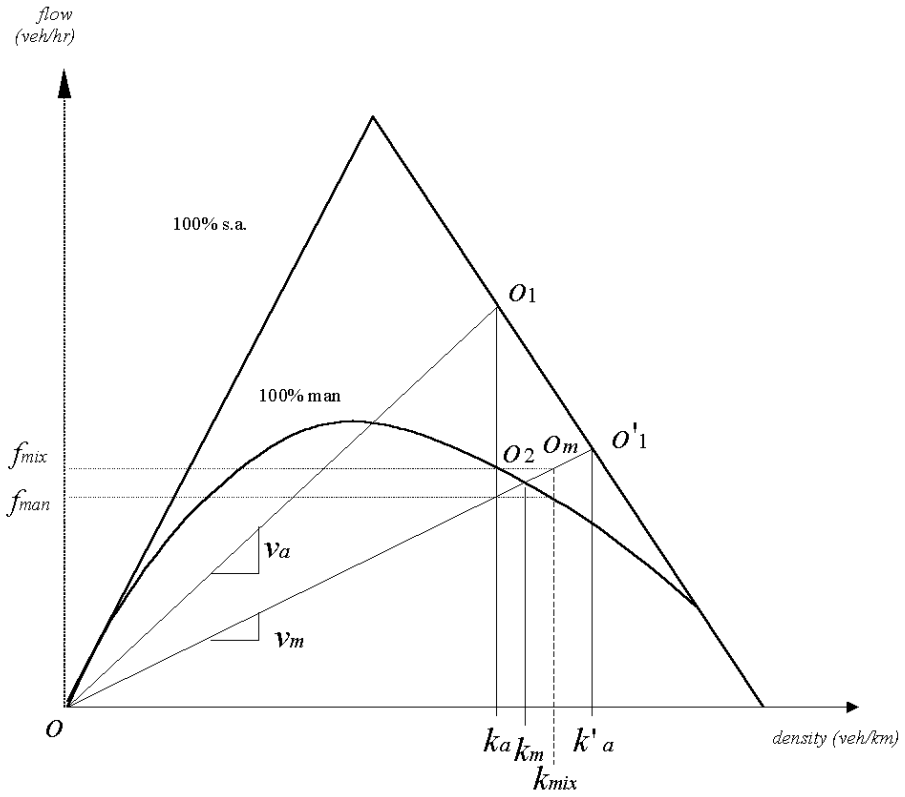

Figure II-4: Derivation of a mixed traffic $q-k$ operating point when the manual vehicles set the average steady state speed.

This means that the average steady state mixed traffic speed is $v_{mix} = v_m$. Now the intervehicle spacing followed by the semi-automated vehicles is given by

$$s_a = h_a v_a + L \tag{18}$$

and the corresponding density is $k_a = \frac{1}{s_a}$, which is the point o_1 in the fundamental diagram in Fig. II-4. Likewise, the intervehicle spacing for the manual vehicles is given by

$$s_m = h_m v_m + L \tag{19}$$

and the density is $k_m = \frac{1}{s_m}$, the point o_2 in the fundamental diagram. Now as the total traffic travels at average speed v_m, then (18) changes to

$$s_a' = h_a v_m + L \tag{20}$$

and the new density is given by $k_a' = \frac{1}{s_a'}$, which corresponds to the point o_1' in the fundamental diagram. The density of the mixed traffic by Remark 1 always satisfies

$$k_m < k_{mix} < k_a \tag{21}$$

Thus the new point in the fundamental diagram of mixed traffic is given by o_m corresponding to mixed traffic flow rate f_{mix}.

Consider now 100% manual traffic at density k_{mix}. The manual traffic flow rate corresponding to that density is given by $f_{man} < f_{mix}$. Thus we show that the mixed traffic flow rate is greater than the manual traffic flow rate for the same traffic density when the manual vehicles set the average mixed traffic speed at steady state.

Case 2: $v_a < v_m$

This means that the average steady state mixed traffic speed is $v_{mix} = v_a$. Now the intervehicle spacing followed by the semi-automated vehicles is given by

$$s_a = h_a v_a + L \tag{22}$$

and the corresponding density is $k_a = \frac{1}{s_a}$, which is the point o_2 in the fundamental diagram in Fig. II-5. Likewise, the intervehicle spacing for the manual vehicles is given by

$$s_m = h_m v_m + L \tag{23}$$

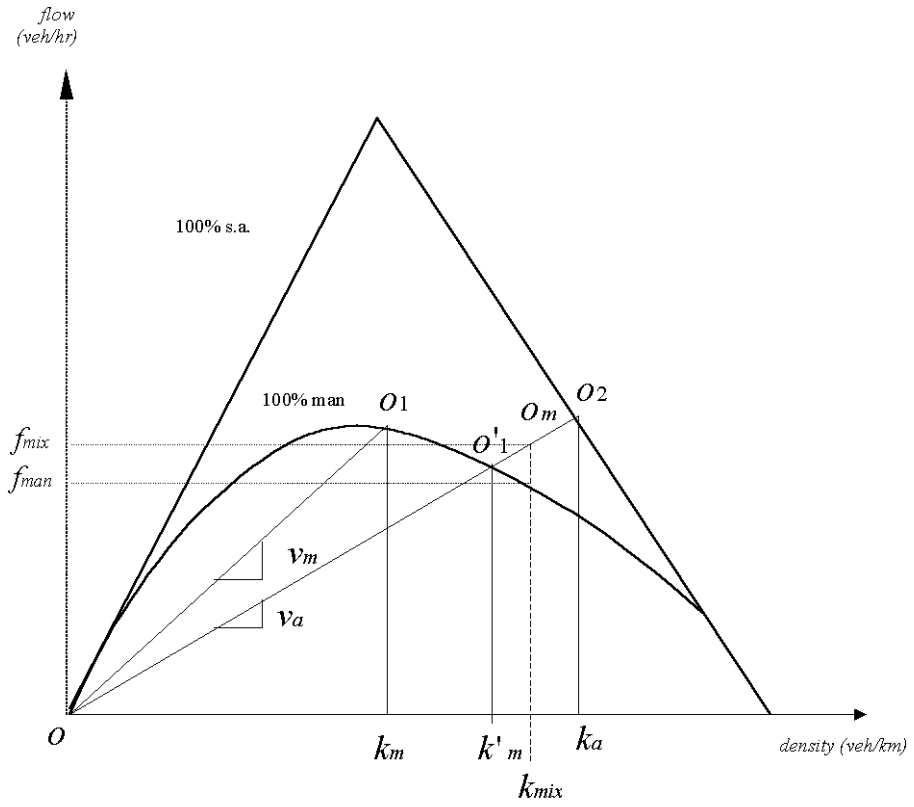

Figure II-5: Derivation of a mixed traffic $q-k$ operating point when the semi-automated vehicles set the steady state average speed.

and the density is $k_m = \frac{1}{s_m}$, the point o_1 in the fundamental diagram. Now as the total traffic travels at average speed v_a, then (23) changes to

$$s'_m = h_m v_a + L \tag{24}$$

and the new density is given by $k'_m = \frac{1}{s'_m}$, which corresponds to the point o'_1 in the fundamental diagram. Using Remark 1 and (21) we show that mixed traffic point is given by o_m corresponding to mixed traffic flow rate f_{mix}.

Consider now 100% manual traffic at density k_{mix}. The manual traffic flow rate corresponding to that density is given by $f_{man} < f_{mix}$. Thus we show that the mixed traffic flow rate is greater than the manual traffic flow rate for the same traffic density when the semi-automated vehicles set the average mixed traffic speed at steady state.

Case 3: $v_a = v_m$

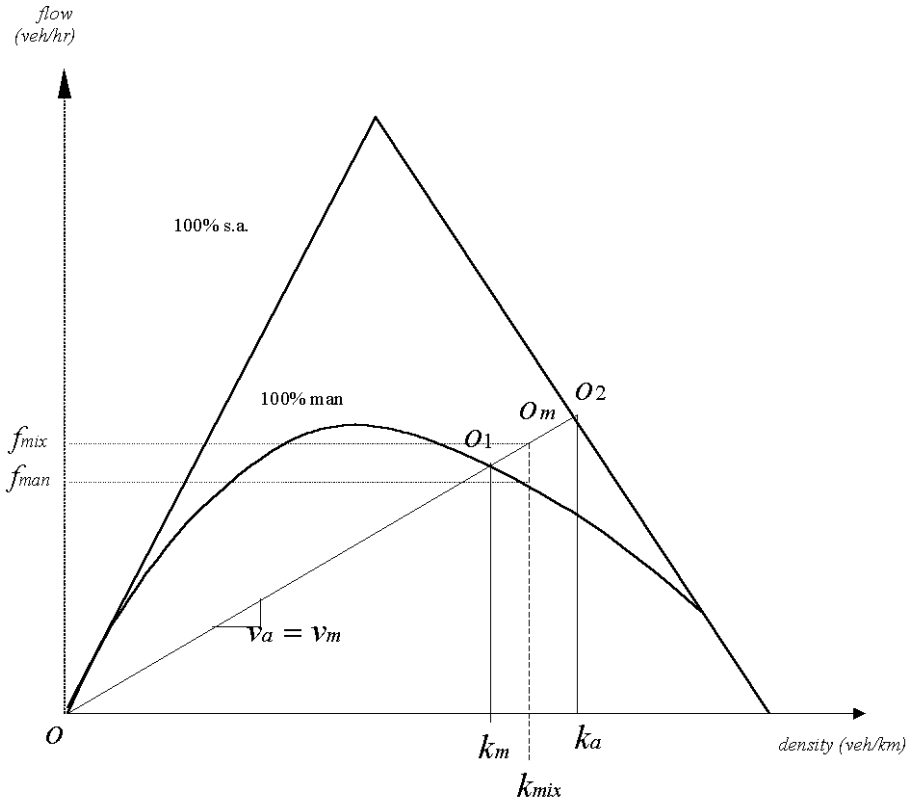

Figure II-6: Derivation of a mixed traffic $q-k$ operating point when the average speed of the semi-automated and the manual vehicles are the same at steady state.

This means that the average steady state mixed traffic speed is $v_{mix} = v_a = v_m$. Now the intervehicle spacing followed by the semi-automated vehicles is given by

$$s_a = h_a v_a + L \tag{25}$$

and the corresponding density is $k_a = \frac{1}{s_a}$, which is the point o_2 in the fundamental diagram in Fig. II-6. Likewise, the intervehicle spacing for the manual vehicles is given by

$$s_m = h_m v_m + L \tag{26}$$

and the density is $k_m = \frac{1}{s_m}$, the point o_1 in the fundamental diagram. Now as the total traffic travels at speed $v_a = v_m$, the operating point of the mixed traffic flow is given by o_m corresponding to mixed traffic density $k'_m = \frac{1}{s'_m}$ and mixed traffic flow rate f_{mix}.

Consider now 100% manual traffic at density k_{mix}. The manual traffic flow rate corresponding to that density is given by $f_{man} < f_{mix}$. Thus we show that the mixed traffic flow rate is greater than the manual traffic flow rate for the same traffic density when the average speed of the semi-automated vehicles and the manual vehicles are the same at steady state.

Lemma 1 and its proof give an insight into the evolution of mixed traffic. To observe the behavior of the mixed traffic $q-k$ curve operating point as the percentage p of semi-automated vehicles increases, we consider two separate cases:

Case 1 Assume that as p increases, the average speed is equal to the speed of the manual vehicles and $k_a \le k_{ca}$. Then from (7) as the percentage of semi-automated vehicles increases, i.e. $p \to 1$, $k_m = k \to 0$ and $v \to v_f$. From (17) $k_{mix} \to k_a$ to give us

$$q = \lim_{p \to 1} k_{mix} v = k_a v_f \tag{27}$$

This is the same as (15) for $k_a \le k_{ca}$.

Case 2 Assume that as p increases, the average speed is equal to the speed of the semi-automated vehicles. This means that $k_a > k_{ca}$. Otherwise the average speed of semi-automated vehicles will be v_f, the maximum for manual vehicles, which is not possible. Then from (14) as $p \to 1$, $v \to \frac{1}{h_a}\left(\frac{1}{k_a} - L\right)$ and from (17) $k_{mix} \to k_a$ to give us

$$q = \lim_{p \to 1} k_{mix} v = \frac{1}{h_a}(1 - k_a L) \tag{28}$$

This is the same as (15) for $k_a > k_{ca}$.

Thus we observe how the $q-k$ curve for mixed traffic converges to the $q-k$ curve for 100% semi-automated traffic as the percentage of semi-automated vehicles increases.

Now we draw a $q-k$ curve for a given market penetration of semi-automated vehicles with the help of the analyses presented above. The initial points of the curve merge with the $q-k$ curves for 100% semi-automated and 100% manual traffic as seen in Fig. II-7, denoting the region where all vehicles travel at mean free speed and there is no vehicle-to-vehicle interaction. Thereafter we trace the bivariate relationship for mixed traffic using the average intervehicle spacings used by the manual and the semi-automated vehicles as outlined previously. Each unique p corresponds to a unique mixed traffic $q-k$ curve.

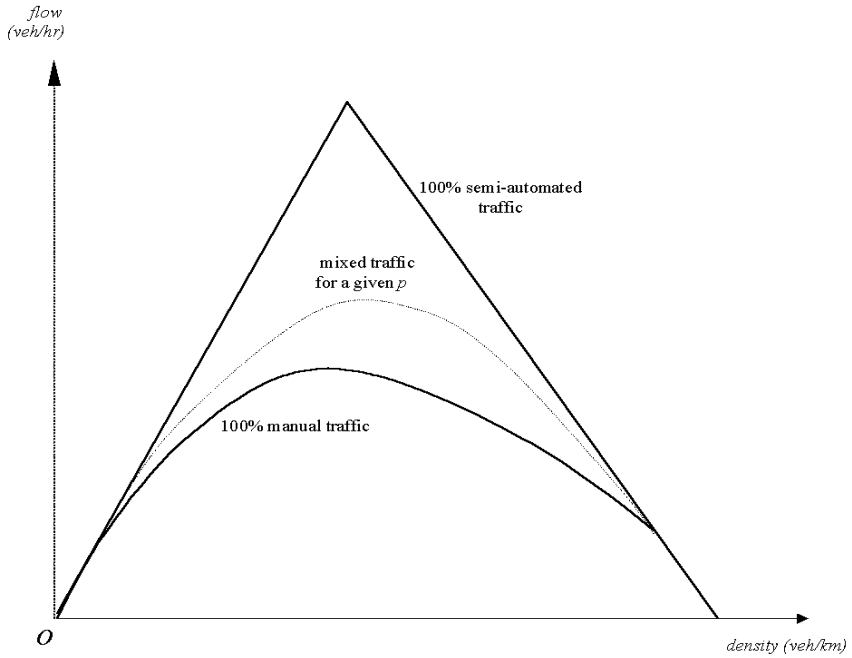

Figure II-7: Fundamental $q-k$ diagrams for 100% semi-automated, 100% manual and *p* mixed traffic at steady state conditions.

Lastly, we investigate the mixed traffic critical density. Each curve has a maximum traffic flow point that corresponds to the critical density. Therefore, the mixed traffic critical density depends on the combination of the intervehicle spacings s_a and s_m used by the semi-automated and the manual vehicles, respectively. Furthermore, the operating point on the $q-k$ curve at critical density corresponding to maximum mixed traffic flow is expected to be unstable and lead to a breakdown in mixed traffic flow. Since at critical density there are no available gaps left, a phenomenon similar to that observed in manual traffic is expected to occur in the event of a traffic disturbance.

II-3 Shock Waves in Mixed Traffic

Shock waves are discontinuous waves that occur when traffic on a section of a road is denser in front and less dense behind. The waves on the less dense section travel faster than those in the dense section ahead and catch up with them. Then the continuous waves

coalesce into a discontinuous wave or a 'shock wave' [1]. It can be shown that shock waves travel at a speed given by

$$u = \frac{\Delta q}{\Delta k} \tag{29}$$

where Δq and Δk are the traffic flow rate and traffic density differences, respectively, between the two sections. In the fundamental diagram for manual traffic, this is given by the slope of the chord joining the two points that represent conditions ahead and behind the shock wave at *a* and *b*, respectively (Fig. II-8).

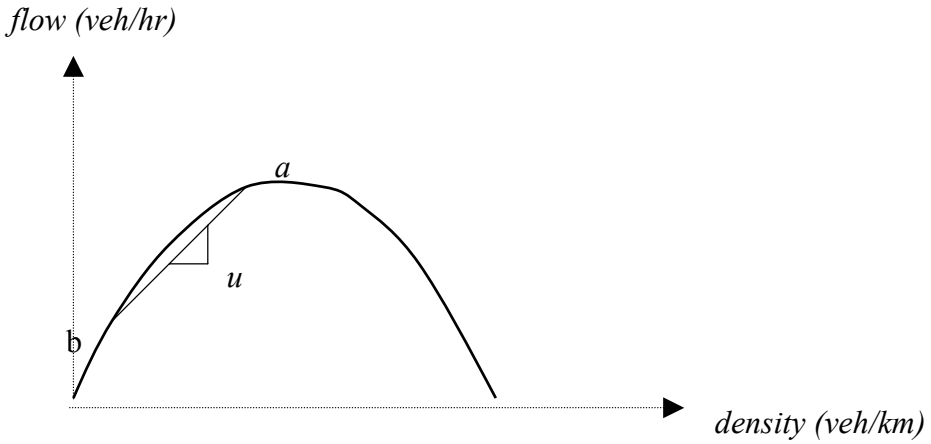

Figure II- 8: Shock wave in manual traffic.

The question that we pose is: how does the mixing of semi-automated and manual vehicles affect the shock waves? We answer the question using space-time diagrams that represent vehicle trajectories. This simple theory of traffic evolution will provide an insight into the effect of semi-automated vehicles among manually driven ones on the propagation of shock waves. The theory is also used in [4] and is a version of one originally developed in [1]. It is presented in a graphical way and assumes the following: no overtaking and vehicles of the same class (i.e. manual and semi-automated) exhibit identical headways, spacings and velocities within a given state.

Figure II- 9(a) shows the space-time graph for 5 vehicles in manual traffic. At time instant t_d there is a disturbance that causes the lead vehicle to slow down, denoted by a change in slope in the diagram. We assume that the vehicle decelerations occur instantaneously. After a time lag τ, the following vehicle reacts and decelerates to maintain the intervehicle spacing depending on a constant time headway policy.

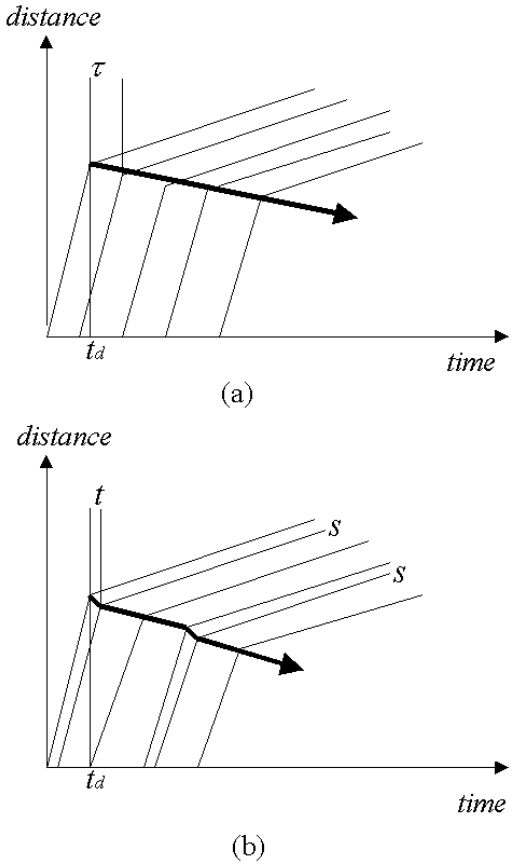

Figure II- 9: Space-time graph showing traffic evolution and the propagation of shock waves in (a) manual traffic and (b) mixed traffic.

Likewise, the rest of the manual vehicles respond as shown. The shock wave that exists at the boundary of the two regions moves back at a speed given by the slope of the arrow in Fig. II-9(a).

For mixed traffic shown in Fig. II-9(b), the lines marked 's' denote semi-automated vehicles while the rest are manually driven ones. As before, the disturbance at t_d causes the first vehicle to slow down. The following semi-automated vehicle reacts after a time t, where t depends on the sensors and the actuators of the semi-automated vehicle and $t << \tau$, i.e. much smaller than the time lag for human drivers in manual vehicles. This effect continues upstream with the semi-automated vehicles reacting almost instantaneously to speed changes while the manual vehicles have a time lag τ. As shown in Fig. II-9(b), the resultant effect is that the average slope of the shock wave increases and as a result it travels upstream at a higher speed than in Fig. II-9(a).

This phenomenon is illustrated in a three-dimensional representation of the space-time diagram. We construct an axis of cumulative number of vehicles at three different distance points and at three different time instances. The surface of the cumulative vehicle count $N(x,t)$ is staircase-shaped, with each step representing a vehicle trajectory.

It follows that if the surfaces are taken to be continuous, then the traffic flow rate at a given point can be obtained from the $N(x,t)-t$ diagrams directly by using

$$q_x(t) = \frac{\partial N(x,t)}{\partial t} \tag{30}$$

and the traffic density at a given time can be obtained from the $N(x,t)-x$ diagrams using

$$k_t(x) = -\frac{\partial N(x,t)}{\partial x} \tag{31}$$

We use a negative sign in (31) because the cumulative vehicle count is considered by counting the number of vehicles that have not yet crossed the line at a time instance *t* in the space-time diagrams. This is the number of vehicles to the left of *t,* which is opposite to the motion of the vehicles and hence the negative derivative.

It is important to note that the continuum approximation to a discrete flow is valid only in the regime of dense traffic. Writing (30) and (31) together, we obtain the continuity equation

$$\frac{\partial q}{\partial x} + \frac{\partial k}{\partial t} = 0 \tag{32}$$

The cumulative vehicle count curve $N(x_2,t)$ for the point x_2 in the $N(x,t)-t$ diagrams in Fig. II-10 is obtained by shifting the curve $N(x_1,t)$ horizontally to the right by the time it takes a vehicle to travel from x_1 to x_2. However, this is not the proper representation of the cumulative curve at x_2 due to the presence of the shock wave. Thus we perform the following transformations. We shift the cumulative curve $N(x_3,t)$ for x_3 (a point after the shock wave) horizontally to the right by the time it takes the shock wave to travel from x_3 to x_2, and vertically upwards by the number of vehicles that cross the shock wave interface. The number of vehicles that cross the shock wave interface is given by the product of traffic density in the region after the shock wave and the distance from x_2 to x_3. This curve is then combined with $N(x_2,t)$ to obtain the correct cumulative curve $N'(x_2,t)$ at x_2. We use a similar procedure to construct the cumulative

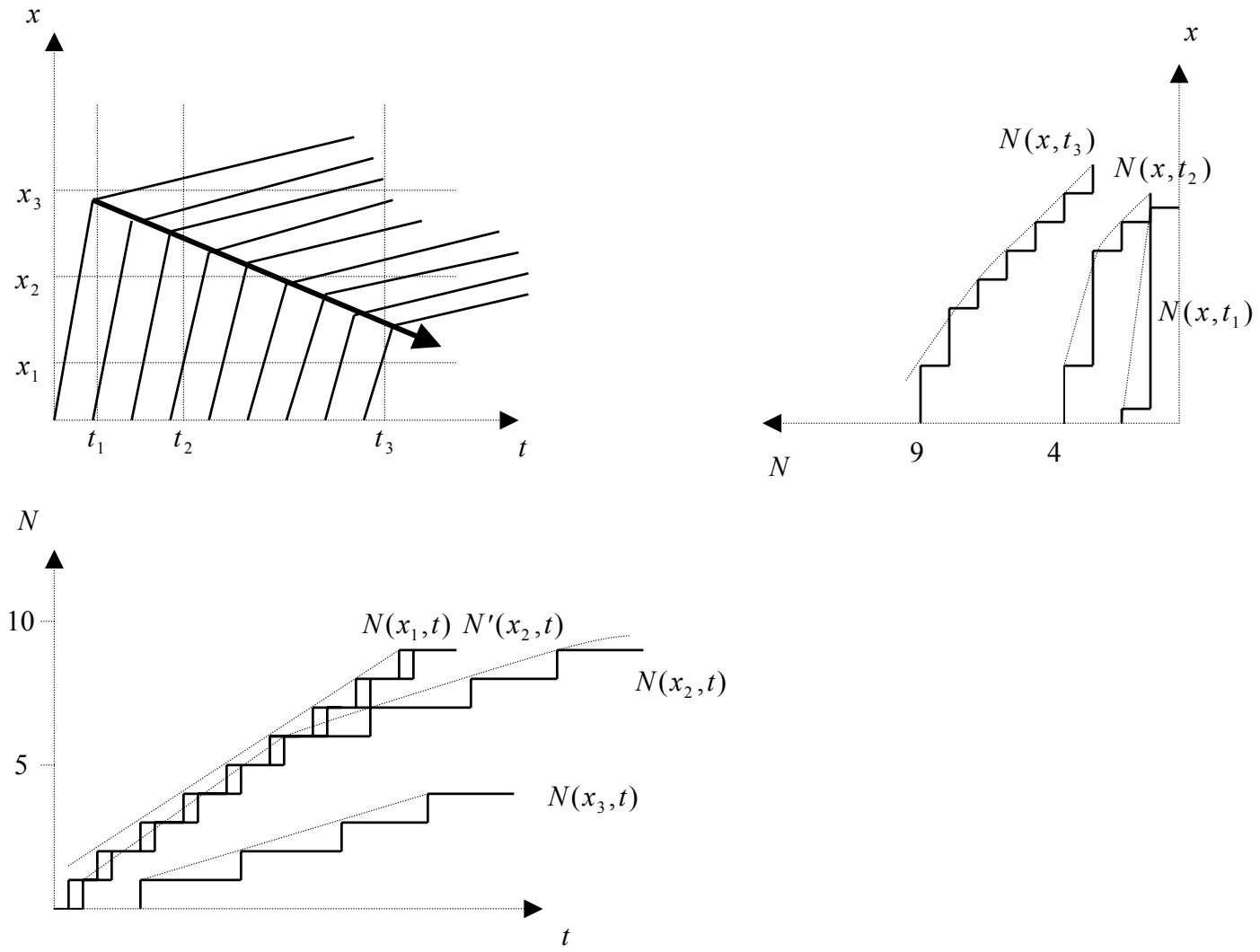

Figure II- 10(a): Three-dimensional representation of manual traffic.

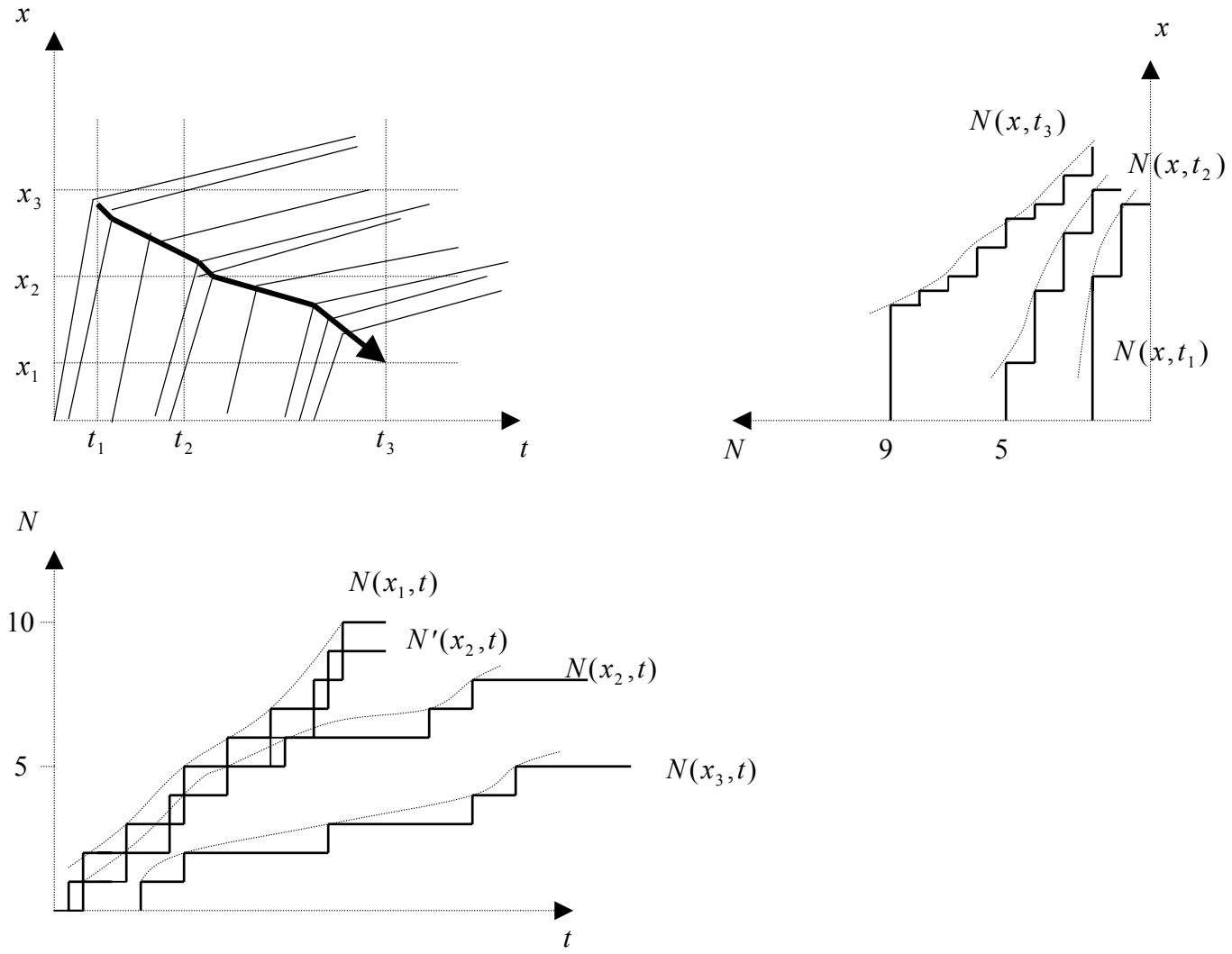

Figure II- 10(b): Three-dimensional representation of mixed traffic.

vehicle count curve $N(x,t_2)$ at time instant t_2 in $N(x,t)-x$ diagrams in Fig. II-10. The cumulative *N*-curves are the ones that will be observed if vehicles counts are taken using measurement devices at positions x_1, x_2 and x_3 at time instances t_1, t_2 and t_3.

We observe from the cumulative curves in Fig. II-10 that the traffic flow rate and the traffic density are greater in mixed traffic than in manual traffic. Furthermore, we observe from the $N(x,t)-t$ diagrams that the traffic flow rate at a given point decreases more rapidly in mixed traffic than in manual traffic. Likewise, from the $N(x,t)-x$ diagrams, we can conclude that the rate of increase in traffic density is higher in mixed traffic than in manual traffic. These are consequences of the shock wave travelling faster in mixed traffic than in manual traffic.

To demonstrate this we perform the following simulations for manual and mixed traffic. Consider a stretch of road of length 2.5 km subdivided into 5 sections of 500m each. A constant traffic flow rate is assumed along the road. The manual vehicle dynamics are modeled using the Pipes linear car-following model from [7,8] and the semi-automated vehicle dynamics are modeled using the ICC design presented in [3]. The Pipes linear car following and the ICC models have been validated using actual vehicle following experiments in [3,20]. All vehicles follow a constant time headway policy. The time headways for the manual vehicles are generated according to a lognormal distribution given in [5] while for semi-automated vehicles they are considered to be 1s. It is important to note that the time headway defined in [5] is the time taken to cover the distance that includes the vehicle length. The maximum value for the manual vehicle time headway is taken as 4s. This is done to make the study applicable to current manual traffic where seldom a vehicle in moderately dense traffic conditions uses a time headway greater than 4s. Fig. II-11(a) shows the time headway of vehicles in 100% manual traffic on the road. Initially all vehicles are travelling at 15m/s. We introduce a disturbance in the 3rd section that lasts for 10s and results in all vehicles in that section to slow down to 5m/s. The traffic density and average speed of each section of the road for 50s are shown in Fig. II-11(b) and II-11(c), respectively. We observe a shock wave developing in section II-3 that causes a pile-up of vehicles.

Next, we assume 50% semi-automated vehicles in mixed traffic that are placed randomly among manually driven vehicles on the road. The time headways for the vehicles are shown in Fig. II-12(a). A similar disturbance is introduced that results in all vehicles in section II-3 to slow down to 5m/s. We observe in Fig. II-12(b) and II-12(c) that the shock wave in section II-3 moves back at a speed higher than that in manual traffic. As a result the vehicle pile-up spills over in section II-2 (Fig. II-12(c)).

We observe that the presence of semi-automated vehicles do not affect the total travel time during traffic disturbances when we compare the space-time graphs of vehicles in manual and mixed traffic in Fig. II-13. The 27th vehicle in mixed traffic starts at approximately the same position as the 20th vehicle in manual traffic, and travels 10.6% (covering 365m) more distance than the latter (covering 330m) in 50s. However, this increase is marginal and is within the modeling error.

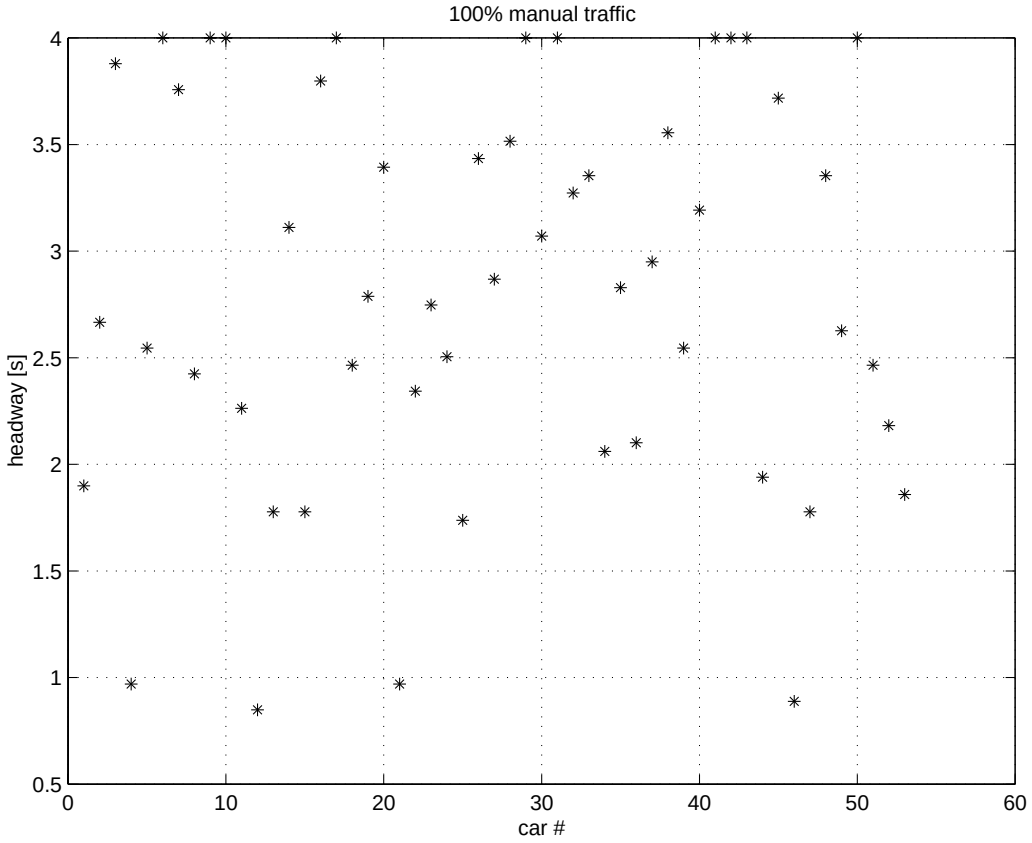

(a)

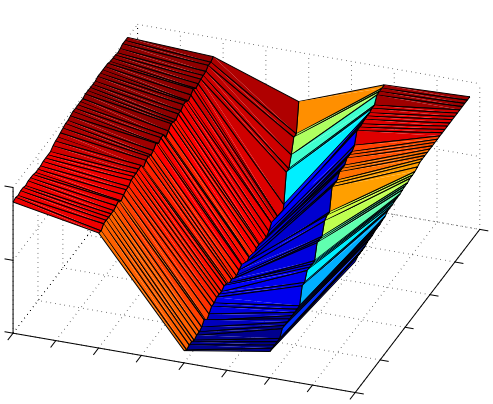

(b)

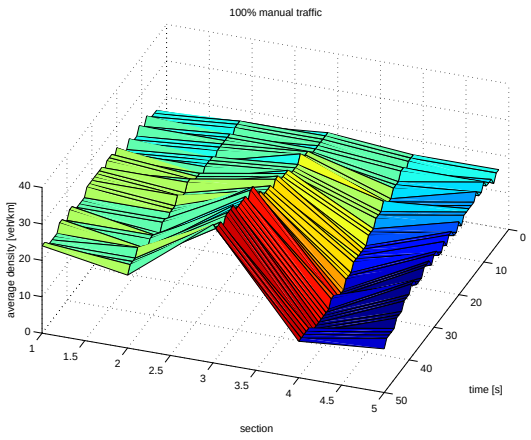

(c)

Figure II- 11: Macroscopic behavior of vehicles in 100% manual traffic.
(a) Time headways of vehicles.
(b) Average speed distribution of vehicles in 5 sections of the highway.
(c) Traffic density distribution of vehicles in the 5 sections of the highway.

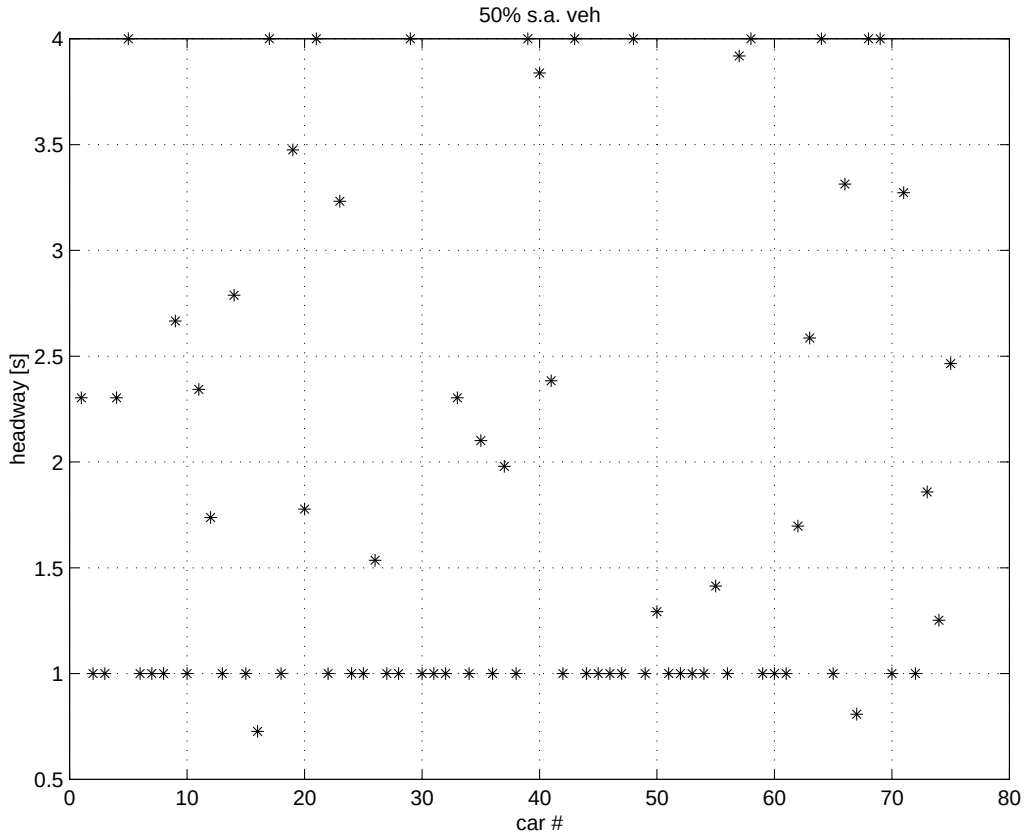

(a)

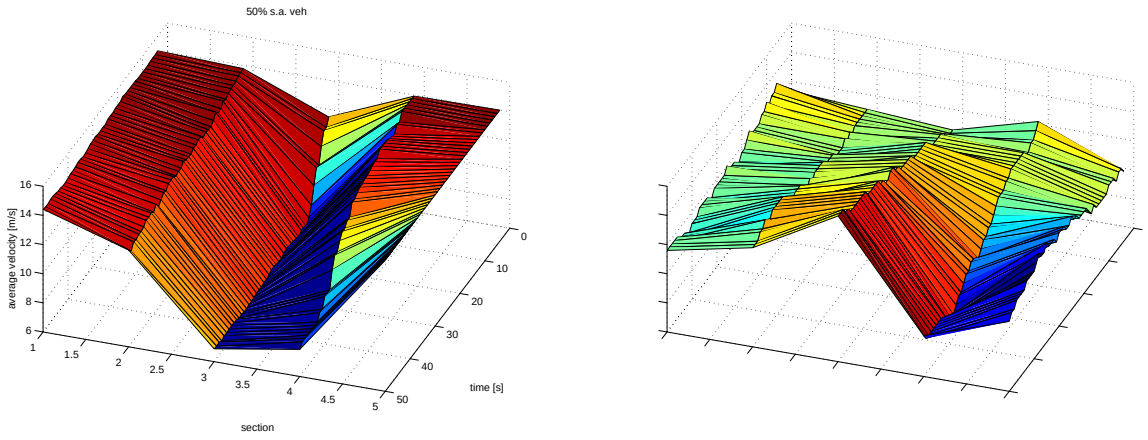

(b) (c)

Figure II- 12: Macroscopic behavior of vehicles in mixed traffic where 50% are semi-automated vehicles.
(a) Time headways of vehicles.
(b) Average speed distribution of vehicles in 5 sections of the highway.
(c) Traffic density distribution of vehicles in 5 sections of the highway.

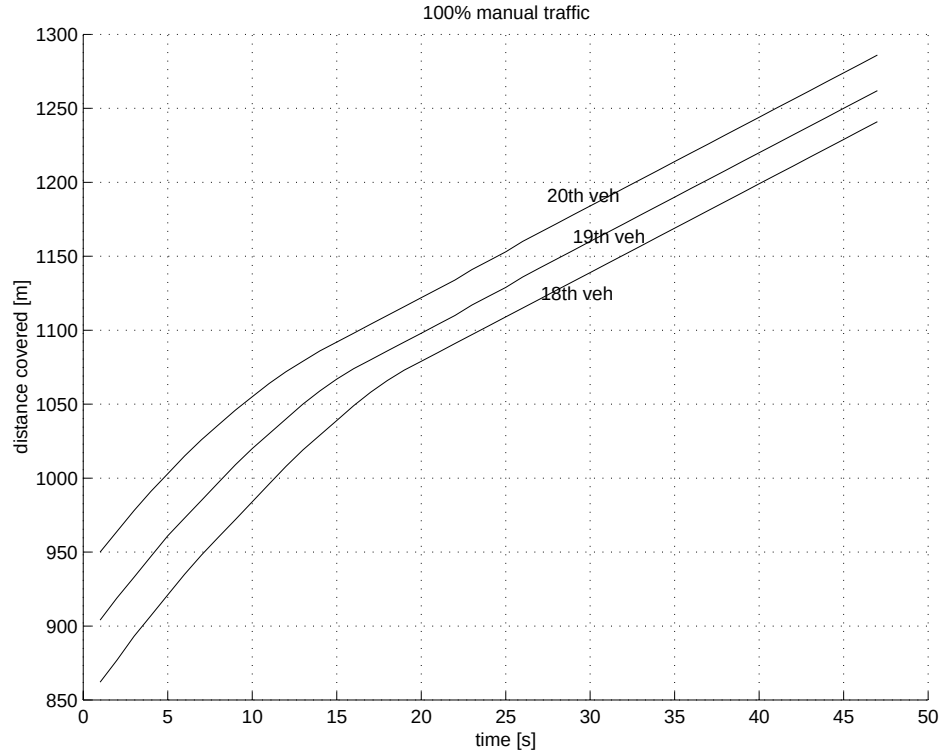

(a)

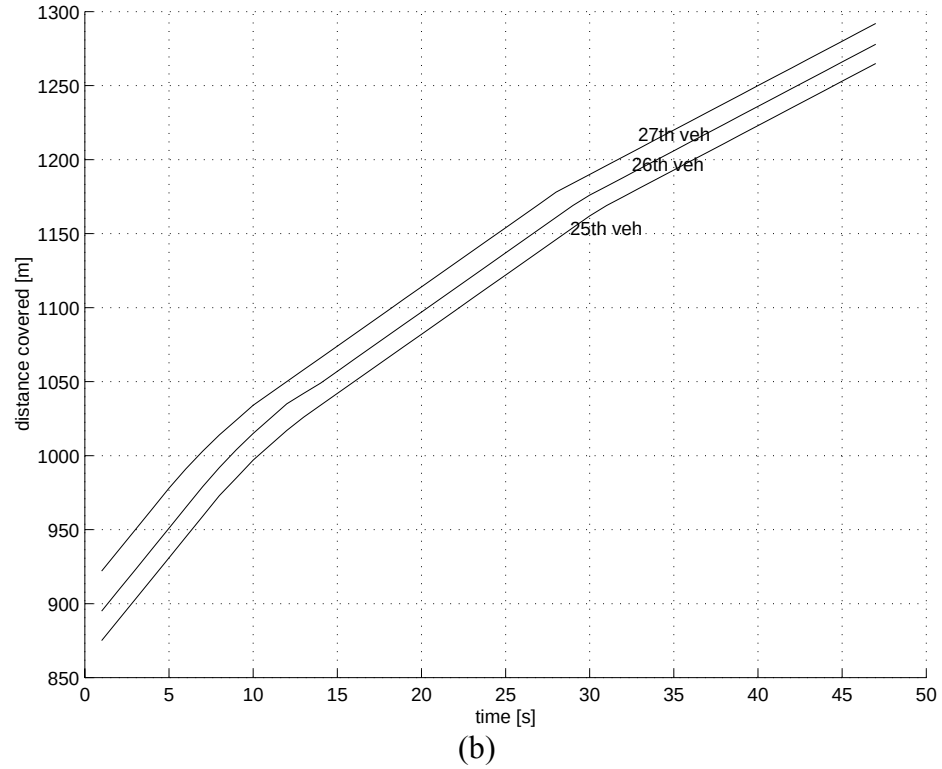

(b)

Figure II- 13: Distance covered by vehicles starting at approximately the same place in (a) 100% manual traffic and (b) mixed traffic with 50% semi-automated vehicles.

II-4 Stop-and-go Traffic

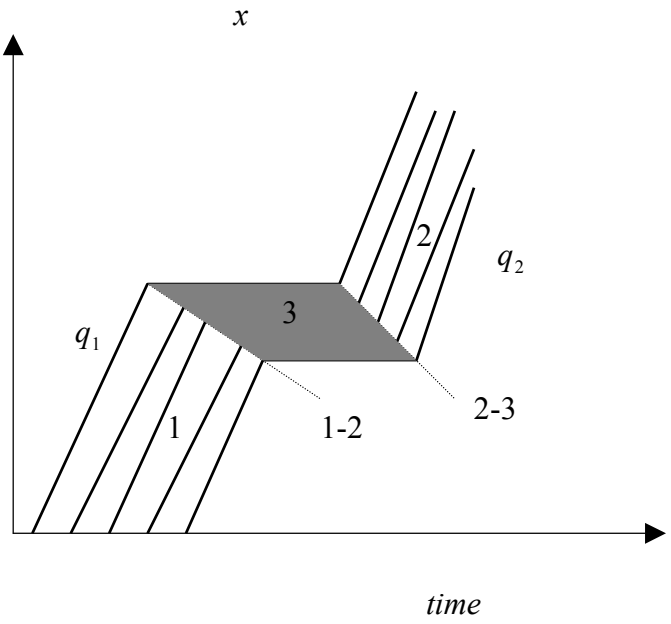

Figure II- 14: Stop-and-go traffic.

In this Section, we show that the average delay experienced by vehicles on the highway due to stop-and-go conditions is shorter in mixed traffic than in manual traffic. Consider Fig. II-14 that shows two shock waves 1-2 and 2-3 that create a stop-and-go condition. The vehicles come to a complete stop after the first shock wave 1-2 as shown in the shaded region 3. Thereafter reaching the second shock wave 2-3 they start moving again. As before, we assume instantaneous acceleration/deceleration of vehicles and vehicles of the same class use identical time headways and spacings at a given state. Consider random vehicle arrivals at the shock wave 1-2 at a rate q_1 per unit time, which is the traffic flow rate in region 1. We take the vehicle discharge rate to be equal to q_2 that represents the traffic flow rate in region 2. The stop-and-go situation can be viewed as a first-come-first-serve system as the first vehicle to stop is the first one to start moving. Therefore we can model the system as an M/M/1 queue with Poisson arrivals and exponential service rate [10]. The theoretical Poisson distribution model is the most commonly used model for vehicular traffic [18,19]. It gives a "satisfactory fit" with empirical traffic data, even at high traffic flow rates as shown in [19].

We have the following arrival and service rates

$$\lambda = q_1 \text{ and } \mu = q_2$$

The utilization factor is given by

$$\rho = \frac{\lambda}{\mu} = \frac{q_1}{q_2} \tag{33}$$

We assume that $q_2 > q_1$, i.e. $\rho < 1$, which is required for ergodicity [10].

II-4.1 Manual Traffic

For manual traffic we have the following:

$q_1 = k_m v_1 = \frac{v_1}{h_m v_1 + L}$, where q_1 is the traffic flow rate in region 1, $k_m = \frac{1}{h_m v_1 + L}$ is the traffic density, h_m is the average time headway in manual traffic, v_1 is the average speed of vehicles in region 1 and L is the average length of vehicles.

$q_2 = k_m v_2 = \frac{v_2}{h_m v_2 + L}$, where q_2 is the traffic flow rate in region 2 and v_2 is the average speed of vehicles in region 2.

Remark 2: For ergodicity, we have

$$q_2 > q_1 \Rightarrow v_2 > v_1 \tag{34}$$

The average delay experienced by a vehicle in region 3 due to the stop-and-go condition is given by [10]

$$T_1 = \frac{1/\mu}{1-\rho} = \frac{1}{q_2 - q_1} = \frac{(h_m v_1 + L)(h_m v_2 + L)}{L(v_2 - v_1)} \tag{35}$$

II-4.2 Mixed Traffic

For mixed traffic we have

$\bar{q}_1 = k_{mix} v_1 = \frac{v_1}{h_{mix} v_1 + L}$, where $\bar{q}_1$ is the mixed traffic flow rate in region 1, $h_{mix} = p h_a + (1-p) h_m$ is the average time headway in mixed traffic, h_a is the time headway of semi-automated vehicles and p is the percentage of semi-automated vehicles in mixed traffic.

$\bar{q}_2 = k_{mix} v_2 = \frac{v_2}{h_{mix} v_2 + L}$, where $\bar{q}_2$ is the mixed traffic flow rate in region 2.

So we have the average delay given by

$$T_2 = \frac{1/\mu}{1-\rho} = \frac{1}{\overline{q}_2 - \overline{q}_1} = \frac{(h_{mix}v_1 + L)(h_{mix}v_2 + L)}{L(v_2 - v_1)} \tag{36}$$

To show that the average delay experienced by vehicles at standstill in region 3 of Fig. II-14 is shorter in mixed traffic than in manual traffic, we need to verify that

$$T_1 - T_2 > 0 \qquad \forall p \qquad p \in (0,1) \tag{37}$$

Using (35) and (36) we obtain

$$T_1 - T_2 = \frac{(h_m v_1 + L)(h_m v_2 + L)}{L(v_2 - v_1)} - \frac{(h_{mix}v_1 + L)(h_{mix}v_2 + L)}{L(v_2 - v_1)} \tag{38}$$

The denominator is always positive by (34). The numerator can be expressed as

$$h_m^2 v_1 v_2 + h_m L(v_1 + v_2) - h_{mix}^2 v_1 v_2 - h_{mix} L(v_1 + v_2) \tag{39}$$

which is always positive for all p as $h_m > h_{mix}$ (since $h_m > h_a$ and $0 < p < 1$). Hence (37) is satisfied.

It is interesting to note that though the above phenomenon occurs, the average number of vehicles at standstill remains unchanged in manual and mixed traffic. It is given by [10]

$$\overline{N} = \frac{\rho}{1-\rho} = \frac{v_1}{v_2 - v_1} \tag{40}$$

which is independent of the average intervehicle spacings and hence the type of traffic.

The above results agree with intuition. In the previous Section we observed that shock waves travel faster in mixed traffic than in manual traffic. Thus the shaded region 3, where the vehicles are at standstill, travels upstream faster in mixed traffic than in manual traffic. This explains (37). However, the relative speed between the two shock waves remains the same in both types of traffic. Thus, the area or the number of vehicles they cover also remains unchanged, which is shown in (40). Furthermore, from the environmental perspective, lower average delay for vehicles in mixed traffic during the presence of shock waves that produce stop-and-go traffic should reduce fuel consumption and air pollution.

II-5 Conclusion

In this Chapter, we derive the $q-k$ diagram for mixed traffic using the $q-k$ diagrams for 100% manual and 100% semi-automated vehicle traffic and assuming that semi-automated vehicles use a time headway smaller than current manual traffic average. We show graphically that semi-automated vehicles propagate traffic disturbances such as shock waves faster without affecting the total travel time. Furthermore, we use an M/M/1 queue to show that the average delay experienced by vehicles in mixed traffic is lower than those in manual traffic during shock waves that produce stop-and-go traffic. Based on the macroscopic mixed traffic analysis presented in this Chapter, we conclude the following results:

- Mixed traffic flow rate is greater than manual traffic flow rate for the same traffic density.
- Mixed traffic $q-k$ curve remains in the region between the $q-k$ curves for 100% manual and 100% semi-automated traffic.
- Presence of semi-automated vehicles in mixed traffic increases the speed of propagation of shock waves without affecting the total travel time.
- Presence of semi-automated vehicles in mixed traffic increases the traffic flow rate and traffic density.
- The average delay experienced by vehicles during stop-and-go conditions is shorter in mixed traffic than in manual traffic while the average number of vehicles at standstill during stop-and-go conditions remains the same in manual and mixed traffic.

References

[1] M.J. Lighthill and G.B. Whitham, "On Kinematic Waves: A Theory of Traffic Flow on Long Crowded Roads", *Proc. of the Royal Society of London,* A229, No. 1178, pp.317-345, 1955.

[2] D.R. Drew, "Traffic Flow Theory and Control", McGraw-Hill Book Co., 1968.

[3] P. Ioannou and T. Xu, "Throttle and Brake Control", *IVHS Journal,* vol. 1(4), pp. 345-377, 1994

[4] M. J. Cassidy, "Traffic Flow and Capacity", *Handbook of Transportation Science,* Ed. Randolph Hall, pp. 151-186, Kluwer Academic Publishers, 1999

[5] S. Cohen, "Traffic Variables", *Encyclopedia of Traffic Flow,* Ed. M. Papageorgiou. Pp.139-143.

[6] A. Bose and P. Ioannou, "Issues and Analysis of Mixed Semi-Automated/Manual Traffic", *SAE Technical Paper Series*, No.981943, 1998

[7] L. A. Pipes, "An Operational Analysis of Traffic Dynamics", *J. of Applied Physics,* vol.24, pp. 271-281, 1953

[8] P. E. Chandler, R. Herman and E. W. Montroll, "Traffic Dynamics: Studies in Car Following", *Operations Research,* vol. 6, pp. 165-184, 1958

[9] R. J. Walker and C. J. Harris, "A Multi-Sensor Fusion System for a Laboratory Based Autonomous Vehicle", *Intelligent Autonomous Vehicles IFAC Workshop*, Southampton U.K., pp. 105-110, 1993.
[10] L. Kleinrock, "Queueing Systems Vol. I: Theory", John Wiley & Sons, 1975.
[11] W. Leutzbach, "Introduction to the theory of traffic flow", Springer-Verlag, 1972.
[12] A. Bose and P. Ioannou, "Analysis of traffic flow with mixed manual and semi-automated vehicles", *Proceedings of American Control Conference*, pp. 2173-2177, 1999.
[13] J.K. Hedrick, D. McMahon, V. Narendran and D. Swaroop, "Longitudinal vehicle controller design for IVHS systems", *Proceedings of American Control Conference,* pp.3107-3112, 1991.
[14] P.A. Ioannou, F. Ahmed-Zaid and D. Wuh, "A time headway autonomous Intelligent Cruise Controller: Design and simulation", Technical Report, USC-SCT 92-11-01, Los Angeles, 1992.
[15] *1985 Highway Capacity Manual*, Transportation Research Board Special Report 209.
[16] I. Chabani and M. Papageorgiou, "Traffic Networks: Flow Modeling and Control", Class notes, MIT, Fall 1997.
[17] L.C. Edie, "Flow Theories", *Traffic Science,* Ed. By D.C. Gazis, John Wiley and Sons, 1974.
[18] D. E. Cleveland and D. G. Capelle, "Queuing Theory Approaches", *An Introduction to Traffic Flow Theory*, Ed. By D. L. Gerlough and D. G. Capelle, Highway Research Board, 1964.
[19] L. C. Edie, "Traffic Delays at Toll Booths", *Journal of the Operations Research Society of America*, vol. 2, No. 2, pp. 107-138, May 1954.
[20] A. Bose and P. Ioannou, "Analysis of Traffic Flow with Mixed Manual and Semi-Automated Vehicles", submitted to IEEE Transactions on Intelligent Transportation Systems, 2000.
[21] D. Swaroop and K. R. Rajagopal, "Intelligent Cruise Control Systems and Traffic Flow Stability", *Transportation Research*, *Part C: Emerging Technologies*, 7(6), pp. 329-352, 1999.